R. & M. No. 3494

R. & M. No. 3494

MINISTRY OF TECHNOLOGY

AERONAUTICAL RESEARCH COUNCIL
REPORTS AND MEMORANDA

Wind Tunnel Tests on a Nacelle fitted with Two Lifting Fans in Tandem

By N. Gregory and Edna M. Love

LONDON: HER MAJESTY'S STATIONERY OFFICE
1967
PRICE 15*s.* 6*d.* NET

Wind Tunnel Tests on a Nacelle fitted with Two Lifting Fans in Tandem

By N. Gregory and Edna M. Love

Reports and Memoranda No. 3494
January, 1966

Summary.

Results are given of wind-tunnel tests of a nacelle-shaped body fitted with two lifting fans in tandem. Lift, drag and pitching moment were measured both with the fans installed with axes vertical and also in a modified arrangement with 15 deg rearward tilt. In the latter case, the effects of simple inlet and exit cascades were also examined. The effects of aerodynamic interaction between efflux and mainstream were almost as serious for this slab-sided nacelle as when the same fan was installed in a large wing. The adverse effect on lift was slightly reduced by rearward movement of the fan when only one fan was in use and the other duct sealed, but a greater improvement was obtained when the front fan was used and allowed to induce additional downflow through the open rear duct thus reducing the magnitude of the lower surface suctions.

Five-tube yawmeter traverses in the two vertical fan ducts just above the fans showed much less flow maldistribution at forward speeds compared with the fan in wing because of the 1-diameter length of duct between surface and traverse station. The decay of the cross flow with depth and the effect of variation of one fan rotational speed upon the flow in the other duct were also examined.

LIST OF CONTENTS

*Replaces N.P.L. Aero Report 1185—A.R.C. 27 688.

1. *Introduction.*

Detailed tests of the aerodynamics of a wing with a lifting fan installed have been carried out at N.P.L., and are reported in Reference 1, whilst Reference 2 discusses the effect of forward speed on the flow distribution and performance of the fan. The interaction between the mainstream and the jet efflux, in the presence of a large wing, results in considerable variation through the forward speed range of the lift increment due to the fan, even at constant momentum flux through the fan.

The present tests were therefore planned, in which the same fan would be installed in a 'fuselage' or nacelle of smaller planform area than the wing, i.e. a fairing which would be less liable to induced circulation effects. At the same time, the much greater depth available for the fan installation would allow information to be gathered about the importance of depth of fan location on cross flow and maldistribution at the fan. Further, a modified version could be constructed in which the fan and duct would be tilted 15 deg to the rear.

A second identical fan was also available and so the model was designed for both fans to be installed in tandem. This allowed limited information to be obtained with one fan operative on the effect of fan location, and with both fans working on the effects of one fan upon the other.

Since the work began, results of somewhat similar studies of inflow problems have appeared in References 4 and 5.

2. *Description of Models.*

The nacelle was 10 ft 5 in (3·18m) long overall, and had the two 13·16 in. (0·334m) diameter fans installed, originally on the centreline of the model, with the fan axes at 44 per cent and 58 per cent of the nacelle length from the nose. The nacelle had basically a rectangular cross-section with rounded corners, and tapered to a vertical stern post. The model was of stringer construction with ply cladding and was designed in detail and built by Messrs. Boulton Paul Aircraft Ltd. A general arrangement drawing of the model is given in Fig. 1, and it is shown suspended from the overhead balance of the N.P.L. 13 ft × 9 ft (3·96m × 2·75m) wind tunnel in Fig. 2. The model was supported from the standard struts for the balance which terminate at the mid-height of the working section by means of two unbraced circular struts located 3·5 in (0·089m) ahead of the fan axis and 6 in. (0·152m) below the centreline of the model. As with the previous wing model [1,2], the nacelle was over large for the results to be free from tunnel-constraint effects. The results have only been corrected for the drag of all exposed supports and are uncorrected for tunnel constraint. They may therefore be regarded as being close to what would be obtained in ground effect, since the floor of the tunnel was only 3·3 fan diameters below the bottom of the nacelle, and this omitted correction is likely to be much larger than any of the others.

Shown dotted in Fig. 1 are two cut-out sections containing the intake and exit. These were removable and facilitated inclining the fan axis and altering the vertical position of the fan. They also enabled the fan duct to be altered to a rectangular cross-section at either entry or exit.

The fan units, of 13·16 in (0·344m) diameter with a hub/diameter ratio of $\frac{1}{2}$, are described in detail in References 1 and 2. In the present application they were fitted as standard with a deep inlet boss of elliptical shape and with a long tail cone as shown in Fig. 1. The flow was found to separate about halfway down the tail cone. The two fan axes were $1\frac{1}{3}$ duct (fan) diameters apart and each fan and duct rotates into the 15 deg tilt position about the midpoint of the fan.

Both hub and tail cone were provided with fittings to carry rakes containing three five-tube yawmeters for flow traverses immediately above and below the fan units. The pressure leads were carried outside the tunnel along axial hollow shafts which were used to rotate the yaw heads.

Both perpendicular and tilted fan ducts of circular cross-section were fitted with an inlet flare whose lip radius varied continuously from 0·23 duct diameter (3 in. or 0·076m) at the front of the duct to 0·10 duct diameter (1·35 in. or 0·034m) at the rear. Preliminary tests showed that with this flare, separation of the inflow was avoided for values of V_T/V_F below about 0·28 in both ducts. However, as the forward speed was increased and the extent of separation increased, it was found to have a much larger effect on the fans owing to their greater depth below the surface (1 duct diameter) compared with the fan-in-wing case. The flow conditions were found to be noticeably improved (Section 3) by fitting an *ad hoc*

design of semi-circular slat to the forward half of each duct above the lip as shown in Fig. 1. The semi-circular slats were therefore retained as a standard fitting for tests with vertical ducts, although they were removed for measurements taken in a duct-sealed condition as they protruded above the level of the upper surface.

3. *Force Measurements with Vertical and Tilted Fans.*

Lift, drag and pitching moment were measured over the range of windspeeds between 0 and 60 ft/sec (18·3m/sec) with the nacelle in its standard condition at zero incidence with and without either or both fans rotating at 41·7 rev/sec (which give an efflux velocity in the fan annulus between 90 and 112 ft/sec (27·4 to 34m/sec)). In the cases where the fans were not driven, readings were taken with the appropriate duct either left open or sealed top and bottom with a flush fitting cover. The results are presented in Table 1 and shown plotted in Figs. 3 and 4. Table 1 contains two sets of results used in the subsequent figures, cases with fan driven/duct sealed and duct sealed/fan driven, which were obtained before the advantages of the $\frac{1}{2}$-ring slat were discovered, and which unfortunately were not repeated. It is not thought that these particular measurements are seriously affected in comparing them with the other fan conditions, since the effect of adding the slats in the case of both fans running is shown in Fig. 5 not to be large. The lift is reduced slightly at zero and very low speeds, and is accompanied by a reduced flow through the rear fan, Fig. 15. The lift reduction vanishes at 27 ft/sec (8·2m/sec, or $\mu = 0{\cdot}19$), a speed slightly above that at which, in the absence of the slat, flow separation first occurs upstream of the fan unit. At higher forward speeds a small relative gain in lift is maintained, because the flow separation in the duct which starts at about 40 ft/sec forward speed (12·2m/sec) is less extensive than without the slat. The relative lift gain at higher forward speeds is accompanied by small reductions in drag and pitching moment (Fig. 5), despite the fact that the flow through both fans with slats present is now greater than without the slats (Fig. 15).

The variation of the lift with forward speed depends on the duct condition because when only one fan is driven and the other duct is left open, a flow is induced in the open duct at forward speeds. This flow is an upflow in the front duct when the rear fan is driven, and a downflow in the rear duct when the front fan is driven. This leads to spasmodic reversed windmilling of the front fan at V_T above 40 ft/sec (12·2m/sec) when the rear fan is rotating at 41·7 rev/sec and to rapid rotation of the rear fan at V_T above 25 ft/sec (7·6m/sec) when the front fan is rotating at 41·7 rev/sec.

These force variations are more strikingly displayed in the non-dimensional presentation employed in Figs. 6 and 7. Here, the lift and drag increments above the values measured with both ducts sealed have been divided by the measured momentum flux through both fans at zero forward speed and the variation of these parameters with advance ratio $V_T/\pi nd$ is shown. Advance ratio is used rather than velocity ratio V_T/V_F of the earlier reports as insufficient traverses were carried out to determine fully the effect of forward speed and fan duct condition on the flow rates through the ducts whose fans were driven. For this same reason, the lift and drag increments have been non-dimensionalized by dividing them by the *static* value of the momentum flux. The variation of this latter quantity with forward speed conditions is discussed in Section 4 and the mean flow rate is shown in Fig. 15. The flow rates through the fan are but little affected by the fan conditions so that the variations in the static values of $\Delta L/N_\rho A_F V_{F0}^2$ shown in Fig. 6 (and in $\Delta M/N_\rho A V_{F0}^2 l$ shown in Fig. 8) reflect variations in the surface pressures and arears surrounding the duct(s) on which they act rather than in direct momentum flux through the fan itself.

The pitching-moment increment due to fan operation is displayed in the same way in Fig. 8, and in Fig. 9 an alternative presentation is offered which shows the centre of pressure of the lift increment, measured in fan diameters from the point mid-way between the two fan ducts. In this connection it should be noted that the two fan axes are $1\frac{1}{3}$ fan diameters apart. Also, under static conditions, the lift of the front fan acts 0·09 diameters ahead of the fan axis whilst the lift of the rear fan acts 0·52 diameters ahead of the rear fan axis. These results are uninfluenced by the condition of the duct with non-driven fan since induced flow in this duct increases rapidly with speed and affects substantially only the results at high forward speeds. With both fans running together the resultant static lift acts 0·30 diameters ahead of the mid-point. This may well be due to the asymmetry of the intake lip radius.

The above described force measurements reveal interactions between duct flow and mainstream almost as serious as those encountered in the tests of Reference 1 when the same fan was installed in a large wing. The corresponding lift variation on the plain wing is shown for comparison in Fig. 6. The nearly rectangular cross-section of the present model, whose overall width is 1·83 times the fan diameter, results in a considerable extent of horizontal surface surrounding the fan at exit, where the interaction effects are strongest. It is not altogether surprising therefore that the interactions are greater than those found by Hackett[3] in tests of a fan with much closer fitting body of circular cross-section. The importance of these lower surface suctions is also revealed by a traverse taken at an advance ratio, μ, of 0·28 with the rear fan undriven. Although the speed of flow induced in the rear duct is as high as 0·28 of the flow velocity in the front duct, this only contributes an 8 per cent increase to the momentum flux so that the observed 40 per cent increase in measured lift (Fig. 6) is largely due to the much weaker suctions acting on the remaining portions of the lower surface. This is another example where adverse effects due (or partly due) to entrainment may be altered by reducing the entrainment by surrounding a jet (partly or entirely) by a slower moving stream of air.

The drag increment due to fan operation is also seen (Fig. 7) to exceed somewhat the sink drag of the air entering the fans. This can be reduced by inclining the fan axis so that the rearward component of velocity of the air entering the fans is not completely lost. The great depth of nacelle (compared with the wing installation) allowed a 15 deg rearward tilt of the fan ducts to be incorporated (Fig. 1d), and the measurements obtained in this condition are listed in Table 2 and plotted in Figs. 10 and 11. A non-dimensional presentation of the lift and drag increments is given in Figs. 12 and 13 which may be compared with Figs. 6 and 7. The pitching-moment increment, Fig. 14, may be compared with Fig. 8. These curves are given so that comparisons may be made of the general shape of the curves between the cases fan axis vertical and axis tilted, and of the actual values of the results on either graph according to the number of fans running and their disposition. It should be noted, however, that corresponding values in the two cases, fan axis vertical and tilted, should not be compared directly because the results have been non-dimensionalized in terms of a momentum flux which has been calculated from the mean flow rates shown in Fig. 15, obtained by integrations from the fan traverses. The increase in flow rate when the fan is tilted 50 deg occurs even at zero forward speed, and cannot therefore be due to tilt. Part of the discrepancy is due to the presence in the duct in the case of fan axis vertical, of bridge pieces and bearings and two sets of cog wheels, close to the hub boss and tail cone, which were driven by small link chains spanning the duct in order to rotate the traverse gear. This system had been superseded by a torque tube universally coupled to the traverse arm shaft in the case of the tilted fan axis. The difference accounted for about 4 per cent increase in flow through the fan. The force measurements were taken with a clean duct in both cases. A further discrepancy lay in the fact that the traverse and fan positions were different distances from the surface. In the case of the tilted fans the traverse gear was axially only 0·5 fan diameter below the surface with the fan immediately underneath, whilst the corresponding force measurements were made with the fans in the central position of Fig. 1d. On the other hand, the vertical fan traverses and force measurements were made with the fans in the central position and the traverses immediately above, 0·88d below the surface. The remaining 6 per cent increase in measured flow when the fan was tilted in static conditions may therefore be attributed to the improvement in diffuser efficiency with the fan further away from the exit plane. For these reasons, therefore, no further analysis has been made of the force measurements. Suffice it to say that the figures show that 15 deg tilt reveals a worthwhile reduction in drag with little diminution in lift.

4. *Flow Maldistribution due to Forward Speed.*

With the fans in their standard position in the nacelle with the plane of the leading edges of their radial inlet guide vanes 1·05 duct diameters below the surface (Fig. 1a), 5-hole yawmeter traverses were carried out as close as possible to the fan in a plane 0·88 duct diameters below the surface in a variety of conditions. From these measurements, the flow speed and direction in the plane of the traverse have been calculated, and hence by integration, the mean velocity across the traverse plane, and also axial and cross-flow components of momentum.

In Fig. 15 is shown the variation of the mean flow rate through the fan with the advance ratio. In the case of fan axes vertical, this has been shown for both fans, driven at equal speeds, both with and without the half-ring boundary-layer control slat. At high forward speeds, the slat, by eliminating or reducing the extent of flow separation over the forward portion of the lip, increases the flow rate through the fan. The considerable depth of inlet duct above the fan greatly reduces the maldistribution previously found[2] in forward speed conditions when the fan was close to the surface, so that the flow rate continues to increase with forward speed, in distinction to the case of the fan in wing where there is a marked deterioration in fan performance. The front fan flow assists the air entering the rear fan into the axial direction so that at high advance ratios a greater flux is recorded through the rear fan than through the front fan. For comparison, the flow through the front fan when tilted 15 deg aft is also shown, but only the local gradient of this curve should be compared with those of the other curves since as already explained, the level of this curve is above the others on account of reduced blockage in the fan duct, and increased diffuser efficiency due to the high position of the fan in the duct allowing a tail pipe $1{\cdot}7d$ long compared with the figure of $1{\cdot}0d$ for the vertical fans. In this raised position the fan (at $0{\cdot}46d$ below the surface compared with the normal position of $1{\cdot}05d$ for the vertical fan) is closer to the $0{\cdot}20d$ location of the fan in wing [1,2] as far as cross flow is concerned, so that its effectiveness at high advance ratios is wholly due to the reduction in cross flow caused by the 15 deg tilt.

Contours of flow velocity and angle of underturning are shown for the front fan without the half-ring slat at a forward speed ratio V_T/V_F of 0·48 in Fig. 16 and with the slat in position in Fig. 17. The effect of the slat in reducing extent of flow separation on the front lip is apparent. Corresponding curves for the flow through the rear fan (with slat present) are shown in Fig. 18. It is again seen that the front fan exerts a noticeable smoothing effect on the flow through the rear fan. Comparison of Figs. 16 and 17 with Fig. 14a and b of Reference 2, the corresponding contours for the fan in a wing, show a great improvement in flow uniformity for the fan in the nacelle. That this is due to the settling length of duct is shown by Fig. 19 where the decay in cross-flow with increasing traverse depth is illustrated for an advance ratio of 0·35 (V_T/V_F equal to 0·48 approximately). The decay has been plotted both for the fan in its standard position 1·05 diameters below the surface, and also when immediately below the traverse position (an additional depth of $0{\cdot}04d$). In the latter case it is seen that the cross flow is slightly larger. When the fan is in its standard deep position, the experimental results are found to be in good agreement with the theoretical flow into a two-dimensional duct with the same inlet flare radius as in the nacelle. The flow in this case was computed from careful measurements of streamline paths found using a field-plotter and Teledeltos resistance paper. The agreement of the cross-flow measurements in the present three-dimensional intake with two-dimensional predictions occurs because the cross-flow is essentially two-dimensional in character and is almost free from transverse components.

The variation of the proportion of cross-flow to axial momentum with velocity ratio is shown in Fig. 20, both for the fan-in-wing with shallow immersion (traverse at $0{\cdot}11d$) and for the fan in nacelle at standard depth (traverse at $0{\cdot}88d$), together with results at different depths at one forward-speed ratio. A linear variation with forward speed is found. The difference in cross-flow seen when both fans are rotating in tandem compared with the corresponding point in the series with varying depth of traverse when only one fan was driven is not due to the difference in number of fans operating, but is due to the lower position of the hub boss in the case of the traverse at standard depth with both fans running. In the case of varying depth traverses, the hub boss was at the level of the upper surface with the traverse probe interchanged in turn with various packing pieces. The flow contraction in the vicinity of the hub boss causes a big reduction in cross-flow and the resulting flow is more nearly axial the lower the position of the hub boss.

The true effect of one fan upon the other can be seen from Figs. 21 and 22 where at an advance ratio of 0·35 (V_T/V_F equal to 0·48 approximately) for one fan, the effect of change of second fan speed on cross-flow and axial flow momentum through the first fan is shown. This is given for both front and rear fans in turn. It will be seen that an increase in front fan rotational speed both increases the axial momentum flux through the rear fan and reduces the proportion of cross-flow, but an increase in rear fan speed has a much smaller effect on the flow through the front fan, and in an adverse sense.

The discussion so far has been in terms of the ratio of cross-flow momentum to axial momentum as this quantity allows an integrated view to be taken of the variation of the underturning angle over the

annulus area. This angle, of course, has its most important effect on fan performance along a transverse diameter where the blade incidence is directly affected. Along a fore and aft diameter the effect is a less serious three-dimensional inflow or outflow. It is instructive to examine what a cross-flow momentum/axial momentum ratio of 0·15, such as is found as an extreme case in Fig. 19 at a forward speed ratio, V_T/V_F, of 0·48 with the vertical-axis fan close to the surface, is worth in terms of blade incidence changes. Comparison of the traverse details with those for a traverse under static conditions reveals incidence changes marked on the velocity triangles shown in Fig. 23. The calculations give excessive values for these incidence changes as they neglect the straightening of the flow between the traverse station and the rotor achieved by the duct and by the low solidity inlet guide vanes. The fan was designed for the rotor blades to operate at zero incidence and the static traverse shows that this was achieved within 2 deg. The relatively small increase in incidence experienced by the advancing blade is due to the considerable increase in axial flow on this side of the rotor associated with the reduced pressure rise required under these circumstances. This blade is in no danger of stalling. The retreating blade experiences a much larger incidence change because the cross-flow velocity is subtracted from the blade speed, and also the axial-flow component is not as large as on the retreating side. The incidence change however is fortunately a reduction and just tolerable, though whether this would be true of a multi-stage compressor is less certain. It is also possible that the inlet guide vanes may have stalled.

When the nacelle was rigged with tilted fans, the half-ring slats were not used as they did not match the inlet flare and so made matters worse. In any case, flow separation did not now occur until a much higher speed ratio than in the case of the duct with vertical axis.

Traverses with tilted fans were in the main confined to the front fan duct with the rear fan sealed, and these were unfortunately spoilt by the strangulation, over a range of azimuthal positions, of a tube connected to the middle yawmeter, which was not spotted at the time of taking the observations. Consequently it has not been possible to plot velocity and direction contours, and the accuracy of the flow rate obtained by integration is suspect to $\pm 1\frac{1}{2}$ per cent. Nevertheless the improvement in the flow can be seen from Table III based on the observations from the inner and outer yawmeter heads, but ignoring velocity reductions experienced by the outer probe in its upstream positions, which were due to the thick boundary layer on the forward lip of the duct. In the cases where the traverses were carried out at an axial distance 0·46d below the surface, the fan was located immediately below at 0·66d. The middle velocity ratio of the tests is close to the value 0·26 at which conservation of horizontal momentum would produce a mean axial flow in the duct. It is clear that even with the fan relatively close to the surface, the fan tilt greatly reduces the amount of cross-flow found at off-design conditions. At the highest advance ratio and with the fan lowered to its standard position (in this case an axial (slant) depth of 1·08d c.f. 1·05d when the fan axis was vertical), the flow distribution remained more nearly uniform and axial than those shown in Figs. 16 and 17 for the fan vertical.

The decay with depth of cross-flow momentum in the tilted duct is shown in Fig. 24 for an advance ratio of 0·35 ($V_T/V_F = 0{\cdot}46$). Although the cross-flow at the surface is much less than in the corresponding case with vertical ducts, Fig. 19. The cross-flow takes almost as long to decay. In the case of the traverse plane 0·5d below the surface (with fan at 0·66d, immediately below the traverse, the effect of variation of speed-ratio on the cross-flow is shown in Fig. 25. A linear variation is found, cross-flow being absent at a value of V_T/V_F equal to 0·29 and the slope being about 17 per cent of the theoretical slope for a traverse at the surface. For the vertical axis, Fig. 19 shows that the traverse at the same depth (with fan immediately below) gives 18·7 per cent of the surface value.

5. *Tests with Inlet and Exit Cascades.*

In order to deflect the jet to the rear with an exit cascade, and to reduce flow maldistribution with an intake cascade, top and bottom inserts containing square apertures at entry and exit were made to fit into the basic nacelle, as it was easier to insert cascades into such shapes. Only a limited amount of work was carried out with these transition pieces and their associated cascades before a succession of mechanical troubles with the gearboxes in the fan drive prematurely terminated the whole experiment.

The transition of duct cross-section from circular to the circumscribing square took place in about 10 in. (0·254m). Whilst this was satisfactory at entry, the resulting diffusion at exit, equivalent to a conical

diffuser with 10 deg semi-vertex angle, was so rapid that separation of the flow occurred in the corners of the square duct and the momentum flux and lift was reduced. Separation still occurred after the initial rate of expansion had been reduced slightly by lowering the hub tail-cone by $4\frac{3}{8}$ in. (0·111m) until it terminated in the plane of the leading edges of the available exit cascade. Flow separation in the lower duct was finally avoided only by both replacing the hub tail-cone by a cylindrical extension which extended right down to the level of the available exit cascade and ended in a blunt base, and also by modifying the transition shape by fitting in the corners of the eventual square with a radius 25 per cent of the duct diameter (or length of side of square). The overall diffusion was then equivalent to that of a 4·2 deg cone, nearly equal to the 5 deg obtained with the original circular duct with streamlined tail cone. The measured lifts at constant fan speed and zero forward speed were also identical, the 10 per cent loss due to fitting the original square transition piece having been recovered.

A cascade of 7 symmetrical blades each 10 per cent thick and with a pitch/chord ratio of 0·55 was inserted in the modified square intake used with 15 deg duct tilt. The blades were articulated at 40 per cent of the chord and the trailing portions were aligned parallel to the axis of the duct whilst the inclinations of the forward portions of the blades were adjustable both individually and in unison. Lift measurements were taken with both fans driven at 41·7 rev/sec, and over the range of advance ratios noted, it was found that the cascade settings indicated in Table 4 gave slightly higher values of lift than other settings.

The optimum lift measurements are shown in Fig. 26 which includes a set of results without cascade. The penalty due to skin friction of the unarticulated cascade is only 1 per cent since the flow over the blades in this condition was largely laminar. When deflected, a much larger penalty would be expected, but Fig. 25 shows that at higher forward speeds the original lift values are regained and exceeded, the improved flow conditions in the fan (at constant rotational speed) more than compensating for blade drag.

Inlet flow traverses were attempted in a plane just below the cascade, but owing to the rotary movement of the traverse probes a large number of readings were lost where the probes entered the cascade blade wakes and so it was not possible to estimate the reduction in extent of underturning achieved by the cascade. This phase of the experiment emphasizes the conclusion drawn earlier[1] that future tests on inlet cascades should be carried out on an '*ad hoc*' rig separate from a complete model, and using traverse gear designed for rectilinear movements the more readily to track (and avoid) the regions of cascade blade wakes. Such tests are now in hand.

Lift, drag and pitching moments were next measured over a range of wind speeds with both fans operating at a rotational speed of 41·7 rev/sec, with the inlet cascades fitted at the optimum angle according to Table 4 and with the exit cascades fitted with the blades at angles to the vertical of 30 deg, 15 deg (parallel to the fan axis) 0 deg and – 15 deg (forward pointing). The results are shown plotted dimensionally in Figs. 27 and 28, where comparison is made with similar measurements taken without the cascades, and also with the fans vertical and circular entry and exit. The increments due to the fan have been rendered non-dimensional in terms of a nominal momentum flux and are plotted against advance ratio in Figs. 29 and 30. In the absence of detailed traverse information a mean velocity V_{F0} of 97·8 ft/sec was taken which was the value measured under static conditions with 15 deg fan duct tilt but with circular intake and exit sections. Comparison of the 15 deg exit cascade result with the appropriate curves in Figs. 12, 13 and 14 suggests that this is probably about the correct momentum flux, but with cascade present the lift increment is reduced at zero and low advance ratios and the drag increment is increased at high advance ratios. Pitching-moment increments are high throughout the speed range.

The ratio of drag increment to lift increment measured under static conditions suggests that the efflux is directed to within 10 per cent of its proper direction by the exit cascade setting, but whether the production of thrust by this means is an economical process demands the sort of analysis attempted in Reference 1, together with measurements of input power. Neither the analysis nor the measurements have been attempted here.

6. *Conclusions.*

Force measurements on a slab-sided lifting-fan nacelle with two fans in tandem (uncorrected for tunnel constraint and therefore roughly equivalent to in ground effect) have revealed interactions comparable

with those experienced in earlier tests with a fan-in-wing. This emphasizes the importance noted by Hackett[3] of a streamline cross-section with a minimum of horizontal area near the fan duct exit.

With only one fan driven, and the remaining duct left open, the results are considerably influenced by the induced flow in the adjacent duct, an adverse upflow in front or an additional downflow behind. With the spare duct sealed, the adverse lift effects at high forward speeds are reduced by a rearward shift of the operating fan, but the drag is increased.

High drag at forward speeds (in excess of intake sink drag) is greatly reduced by 15 deg of rearward duct tilt and is accompanied by only a small reduction in lift. The effect of further control by a deflected exit cascade was examined, but the economy of this device was not assessed.

Flow maldistribution at the fan inlet guide vanes at forward speed can be reduced by tilting the fan and by allowing a long settling length between surface and fan. Qualitative information on the decay of cross-flow momentum is given for the benefit of designers aware of what can be tolerated by their engines. The best method of reducing cross flow is an entry cascade, of which a crude example was tried. Detailed tests of a more sophisticated design will follow on a special rig.

The maldistribution of the flow through the single stage fan used was found to be influenced to a small extent by the flow conditions in the adjacent fan duct. Cross-flow in the rear fan duct was reduced, and axial-flow momentum increased, by an increase in rotational speed of the front fan, but conditions in the front fan duct were less affected by variations in the rear fan speed.

The severe maldistribution present at high forward speeds (e.g. $V_T/V_F = 0{\cdot}5$) with the fan close to the surface led to a large incidence differential between advancing and retreating blades. However, because of the off-loading of the fan at forward speeds, this change took the form of a large reduction of incidence on the retreating blade and only a small increase in incidence on the advancing side. For this particular rig, therefore, stalling of the rotor is not likely to occur, and the problems arising from flow maldistribution are likely to be mechanical in nature, i.e. vibration and fatigue problems.

LIST OF SYMBOLS

ρ	Density
A	Fan annulus area
d	Fan (and duct) diameter
h	Axial depth (of fan or traverse) below surface
l	Length of body
n	Fan rotational speed, rev/sec
V_T	Forward speed
V_F	Mean axial speed of flow through fan
μ	Advance ratio, $= V_T/\pi nd$
N	Number of fans operating
L	Lift
D	Drag
M	Pitching moment
Δ	Increments in above due to opening fan aperture(s) and driving fan(s)
α	Underturning angle
θ	Angle of rearward fan tilt

Suffices

o	Zero speed value
f	Front
r	Rear

Metric equivalents

J	Joule
N	Newton

REFERENCES

No.	*Author(s)*	*Title, etc.*
1	N. Gregory, W. G. Raymer and Edna M. Love	Wind tunnel tests of a wing fitted with a single lifting fan. A.R.C. R. & M. 3457. December, 1964.
2	N. Gregory, W. G. Raymer and Edna M. Love	The effect of forward speed on the inlet flow distribution and performance of a lifting fan installed in a wing. A.R.C. R. & M. 3388. June, 1962.
3	J. E. Hackett	Wind tunnel tests on a streamlined fan-lift nacelle, alone and with wings or underfins fitted. A.R.C. 26 969. May, 1965.
4	U. W. Shaub and E. P. Cockshutt	Analytic and experimental studies of normal inlets, with special reference to fan-in-wing VTOL powerplants. Part A, Analytic investigation. Part B. Experimental investigation. I.C.A.S. Paper No. 64 – 572. Fourth Congress, Paris, 1964.
5	B. I. Tyson	Tests of air inlets for jet lift engines. S.A.E./A.S.M.E. Air Transport and Space Meeting. (April, 1964). Tests to establish flow distortion criteria for lift engines. *J.Aircr.* Vol. 2, pp. 411–417. September, 1965.

TABLE 1

Lift, Drag and Pitching Moments for the Nacelle at Zero Incidence with Fan Axes Vertical.

Duct condition		Windspeed V_T ft/sec	Lift lb	Drag lb	Pitching moment* ft – lb
Front	Rear				
Sealed†	Sealed†	0	0	0	0
		10	0	0·102	0·040
		14	0	0·206	0·034
		20	0·02	0·388	0·055
		30	0·01	0·838	0·048
		40	0	1·422	0·112
		50	0	2·200	0·180
		60	0	3·142	0·211
Open	Open	0	0	0	0
		10	−0·01	0·142	0·056
		14	+0·01	0·286	0·233
		20	0·07	0·628	0·900
		25	0·12	0·940	0·978
		30	0·19	1·55	1·57
		40	0·32	2·63	2·58
		50	0·51	4·08	4·10
		60	0·71	5·78	5·88
Fan running at 41·7 rev/sec†	Sealed†	0	10·00	0·08	8·32
		8	10·31	1·70	9·93
		14	9·84	2·95	13·25
		20	8·89	4·25	15·38
		25	7·91	4·88	17·49
		30	7·32	6·05	20·46
		35	7·00	7·18	23·72
		40	6·50	8·38	26·45
		45	6·04	9·41	29·26
		50	5·42	10·38	31·48
		55	5·02	11·39	33·99
		60	4·82	13·08	37·83
Fan running at 41·7 rev/sec†	Open	0	10·86	−0·02	9·20
		8	11·31	1·69	10·63
		14	11·66	3·34	13·87
		20	11·27	4·66	17·01
		25	10·29	5·81	19·69
		30	9·90	7·56	23·94
		40	9·84	11·59	32·06
		50	11·15	16·92	42·66
		60	12·36	22·67	53·45

TABLE 1 (*contd.*)

Duct condition		Windspeed V_T ft/sec	Lift lb	Drag lb	Pitching moment* ft – lb
Front	Rear				
Fan running at 41·7 rev/sec	Fan running at 41·7 rev/sec	0	19·02	0·11	5·97
		7	19·81	3·15	9·46
		14	20·44	5·48	13·97
		20	18·59	7·58	18·24
		25	17·30	9·31	22·73
		30	16·65	11·21	27·29
		40	16·15	14·64	35·80
		50	16·71	19·46	45·62
		60	17·72	27·28	58·87
Open	Fan running at 41·7 rev/sec	0	10·02	·08	−1·81
		9	10·44	1·93	+0·26
		14	10·38	3·26	3·05
		20	9·35	4·08	5·74
		25	8·73	5·22	8·24
		30	8·76	6·96	11·74
		40	8·62	10·04	17·83
		50	6·43	12·65	23·88
		60	5·78	15·04	30·66
Sealed†	Fan running at 41·7 rev/sec†	0	9·70	0·07	−1·63
		8	10·19	1·95	+0·04
		14	9·97	3·18	3·63
		20	9·05	4·29	6·66
		25	8·73	5·45	9·86
		30	8·85	7·25	13·15
		35	9·01	8·64	16·27
		40	9·06	10·14	19·74
		45	9·06	11·68	22·76
		50	8·38	13·22	25·54
		55	7·71	14·57	29·39
		60	7·36	16·26	32·90

*Measured about point on nacelle axis mid-way between fans.

†The semi-circular slat was not fitted in this condition.

TABLE 2

Lift, Drag and Pitching Moments for the Nacelle at Zero Incidence with Fan Axis Tilted 15 deg to the rear.

Duct condition		Windspeed V_T ft/sec	Lift lb	Drag lb	Pitching moment* ft – lb
Front	Rear				
Fan running at 41·7 rev/sec	Sealed	0	10·48	−2·40	9·13
		8	10·84	−1·45	11·54
		14	10·79	−0·59	13·94
		20	9·71	+0·22	16·36
		25	8·37	0·89	18·17
		30	7·20	1·56	20·43
		35	6·40	2·31	22·48
		40	5·68	3·12	24·77
		45	5·20	4·12	27·25
		50	4·78	5·08	29·72
		55	4·52	6·20	32·51
		60	4·32	7·87	35·58
Fan running at 41·7 rev/sec	Open	0	10·33	−2·42	9·04
		8	10·89	−1·25	12·50
		14	11·11	−0·35	14·47
		20	10·23	+0·81	16·96
		25	9·26	1·73	18·98
		30	8·68	2·77	21·62
		35	7·76	4·01	24·40
		40	7·47	5·47	28·31
		45	7·42	7·00	31·88
		50	7·70	8·75	35·86
		55	8·69	11·69	41·57
		60	10·20	14·54	47·63
Fan running at 41·7 rev/sec	Fan running at 41·7 rev/sec†	0	20·24	−4·10	9·73
		8	20·89	−2·25	14·09
		14	20·94	−0·73	17·13
		20	20·45	+0·83	21·28
		25	19·33	2·19	24·76
		30	17·76	3·77	29·40
		35	16·64	5·16	33·96
		40	15·55	6·56	38·08
		45	15·52	8·30	42·71
		50	15·74	10·15	47·38
		55	15·81	12·18	51·03
		60	16·24	14·44	55·99

TABLE 2—*continued*

Duct condition		Windspeed V_T ft/sec	Lift lb	Drag lb	Pitching moment* ft – lb
Front	Rear				
Open	Fan running at 41·7 rev/sec	0	10·24	−2·37	−0·22
		8	10·76	−1·53	1·17
		14	10·76	−0·69	3·54
		20	9·87	0·29	6·34
		25	8·84	−1·07	8·83
		30	7·81	1·92	11·51
		35	7·11	2·90	14·00
		40	6·91	4·18	16·96
		45	6·95	6·00	19·01
		50	7·00	7·37	21·07
		55	7·33	9·21	24·19
		60	7·33	11·04	26·43
Sealed	Fan running at 41·7 rev/sec	0	10·27	−2·37	−0·37
		8	10·84	−1·62	0·79
		14	10·81	−0·45	4·15
		20	9·75	+0·48	7·49
		25	8·56	1·35	10·50
		30	7·97	2·18	13·14
		35	7·34	3·08	15·84
		40	7·08	4·45	18·73
		45	7·20	5·95	21·99
		50	7·41	7·65	24·23
		55	7·42	9·13	27·20
		60	7·47	11·43	30·31

*Measured about point on nacelle axis, midway between fans.

TABLE 3

Fan condition	h/d	V_T ft/sec	μ	V_T/V_F	Range of V_F, ft/sec	Range of α
15 deg tilt	0·46	0	0	0	$95 < V_F < 103$	$-6 \text{ deg} < \alpha < +2 \text{ deg}$
15 deg tilt	0·46	30	·21	0·28	$103 < V_F < 109$	$-2 \text{ deg} < \alpha < +1 \text{ deg}$
15 deg tilt	0·46	50	·35	0·46	$104 < V_F < 116$	$-2 \text{ deg} < \alpha < +4 \text{ deg}$
15 deg tilt	0·92	50	·35	0·46	$107 < V_F < 114$	$-3 \text{ deg} < \alpha < +3 \text{ deg}$
Vertical	0·88	50	·35	0·49	$92 < V_F < 116$	$-10 \text{ deg} < \alpha < +10 \text{ deg}$

TABLE 4

V_T, ft/sec	μ		Optimum Cascade Setting						
			Angle of forward blade to vertical						
0 – 15	0 – 0·105	A	30 deg,	25 deg,	20 deg,	15 deg,	10 deg,	5 deg,	0 deg
20 – 35	0·14 – 0·24	B	35 deg,	30 deg,	25 deg,	20 deg,	15 deg,	10 deg,	5 deg
40 – 60	0·28 – 0·42	C	40 deg,	35 deg,	30 deg,	25 deg,	20 deg,	15 deg,	10 deg

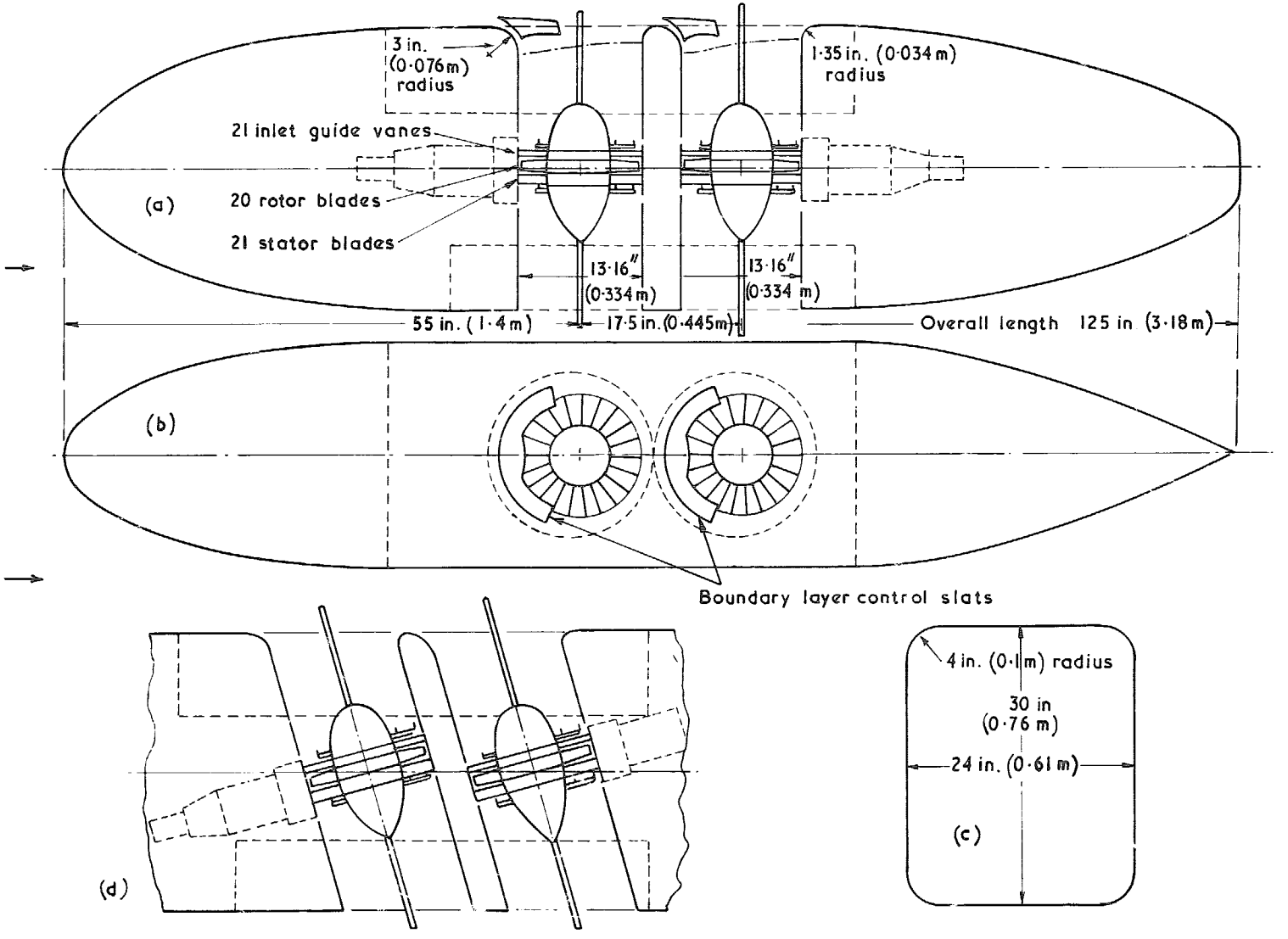

FIG. 1. (a) Centreline section of elevation, and (b) plan view of twin fan nacelle (c) Maximum cross-section (d) Part centreline section of elevation with fans at 15 deg tilt.

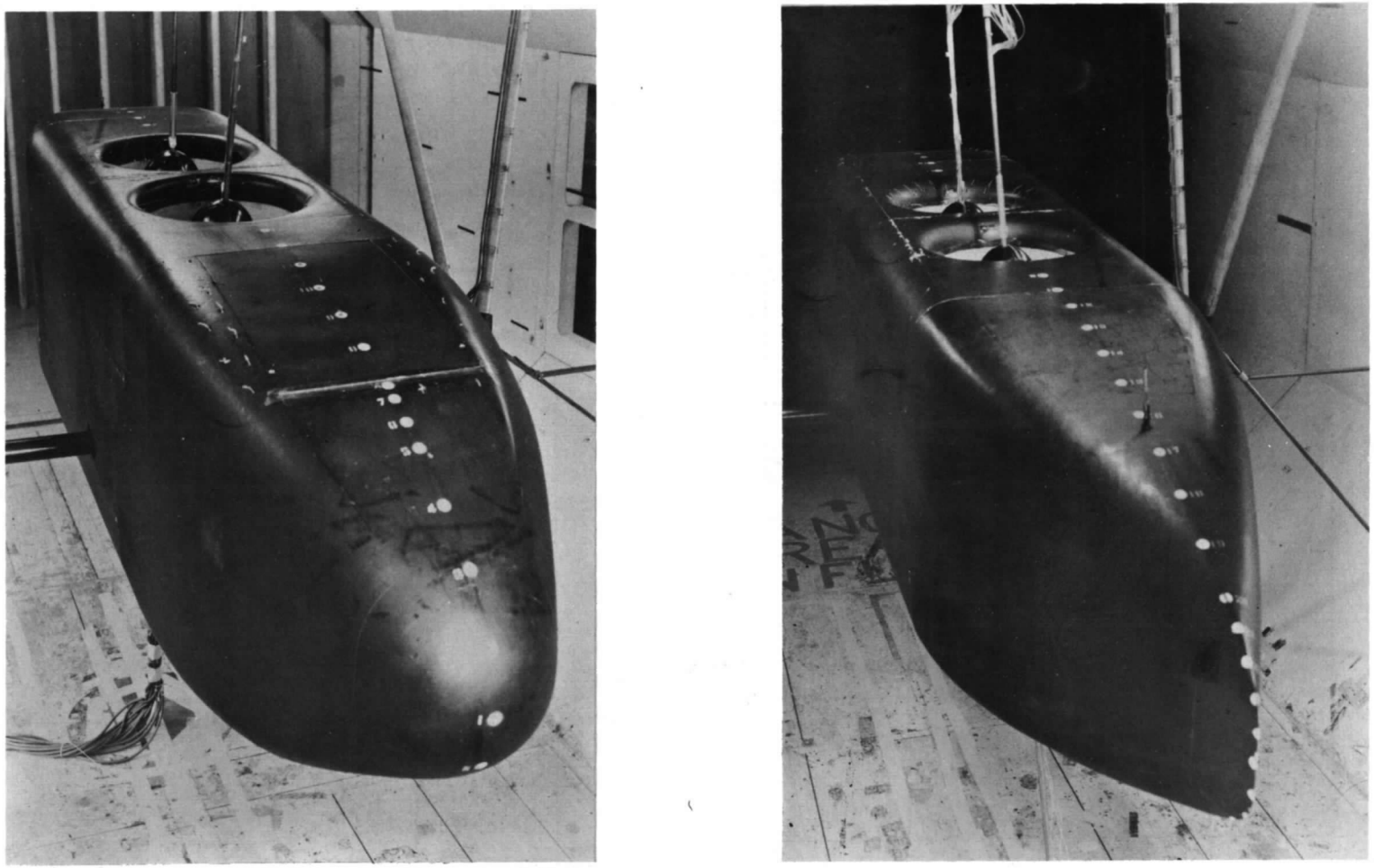

FIG. 2. (a) $\frac{3}{4}$ front view, and (b), $\frac{3}{4}$ rear view of twin-fan lifting nacelle model, with fans in 15 deg tilt position, installed in N.P.L. 13 ft x 9 ft (3·96m $\times$ 2·75m) wind tunnel.

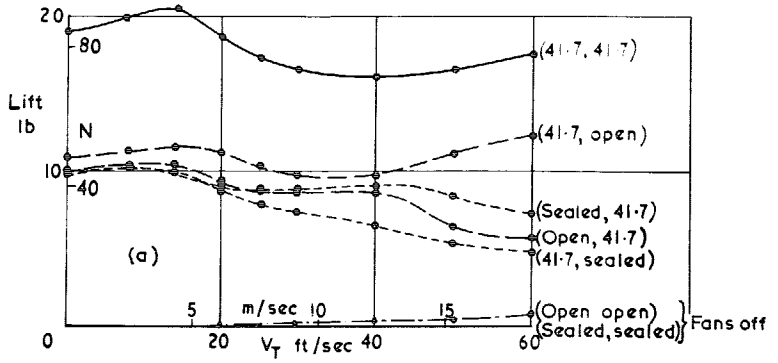

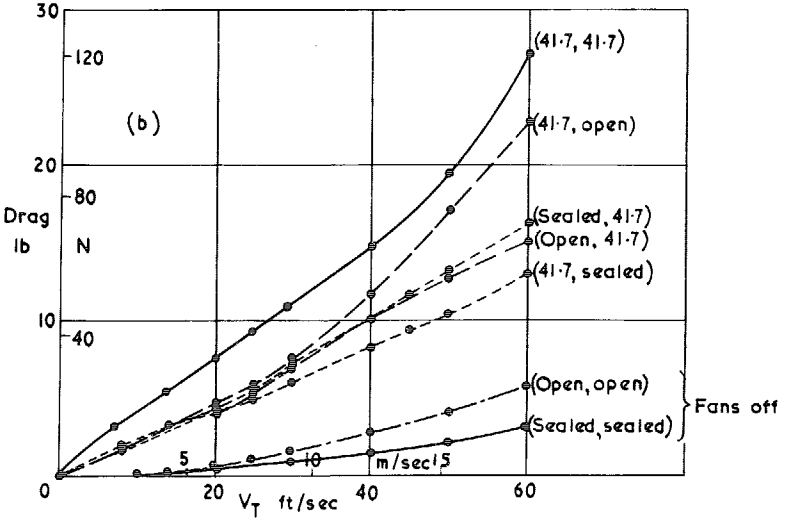

FIG. 3. Variation of (a) lift and (b) drag with forward speed for various duct flow conditions. Fans either driven at 41·7 rev/sec, not driven, or duct sealed. Labels attached to curves indicate condition of front fan and rear fan in order.

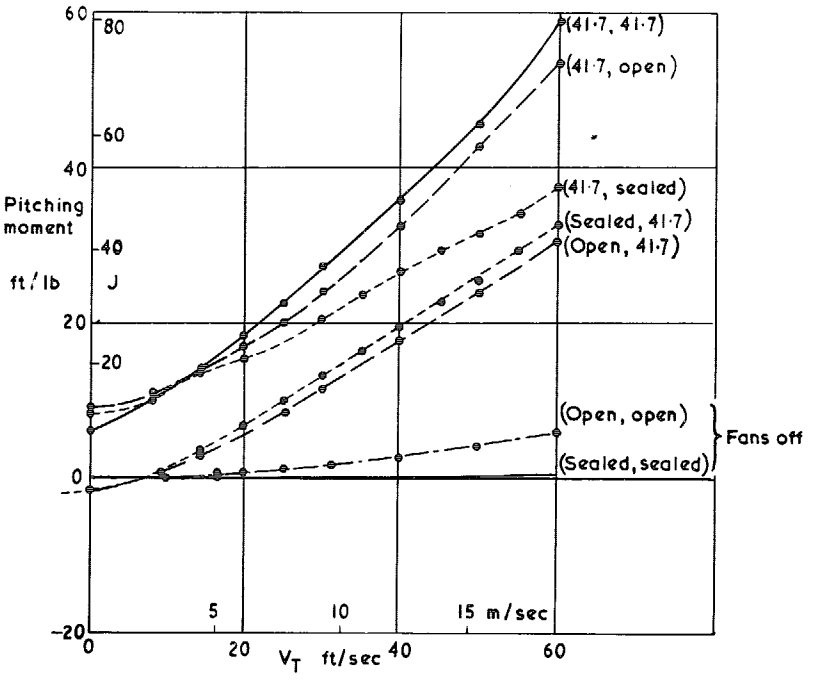

FIG. 4. Variation of pitching moment with forward speed for various duct flow conditions. Fans either driven at 41·7 rev/sec, not driven, or duct sealed.

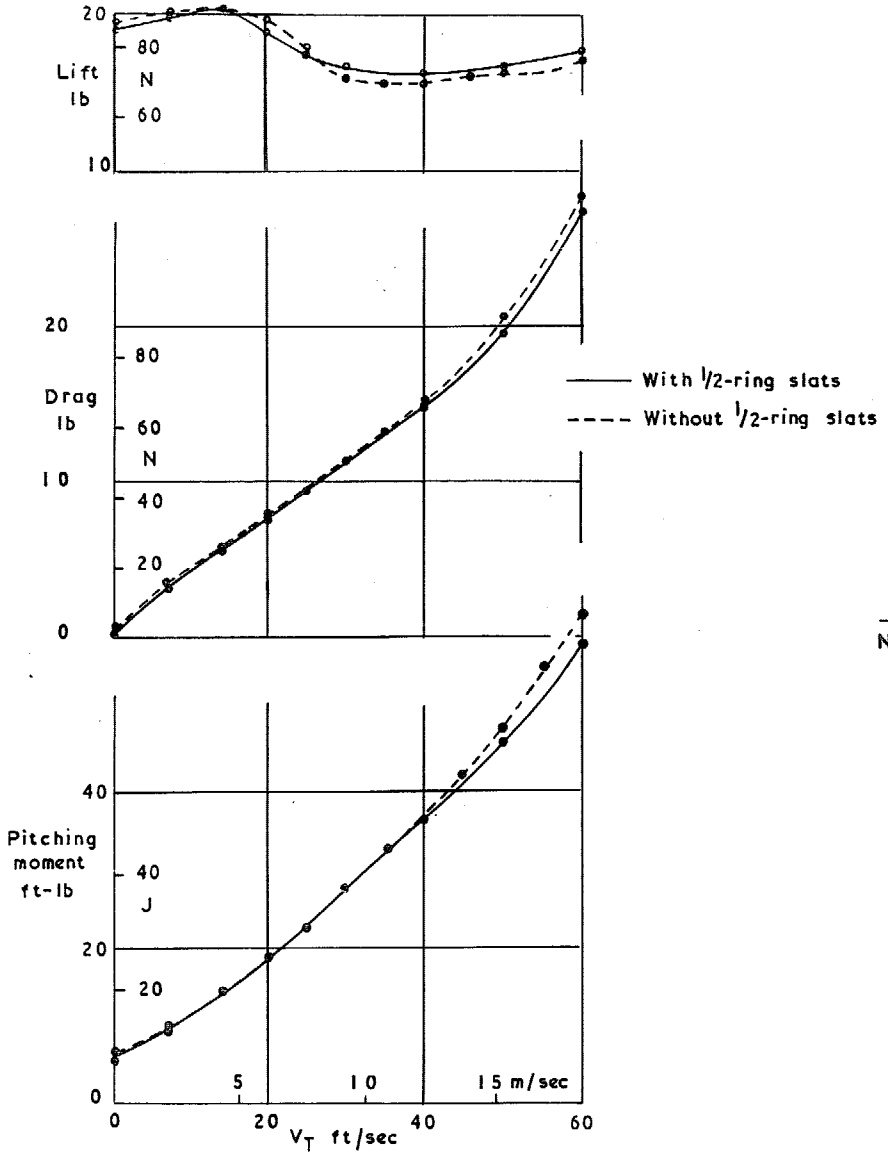

FIG. 5. Effect of adding half-ring slat on the variation of lift drag and pitching moment with forward speed. Both fans driven at 41·7 rev/sec.

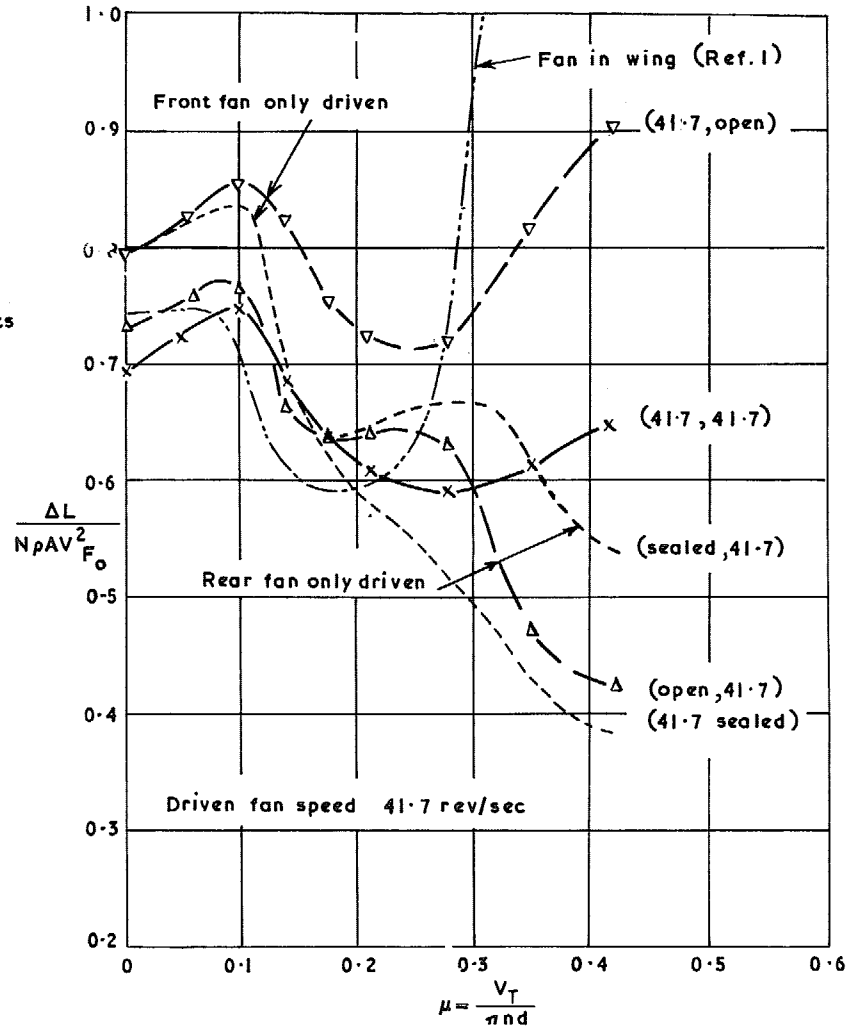

FIG. 6. Variation with advance ratio of the lift increment due to the fans measured as a proportion of the corresponding momentum flux at zero forward speed.

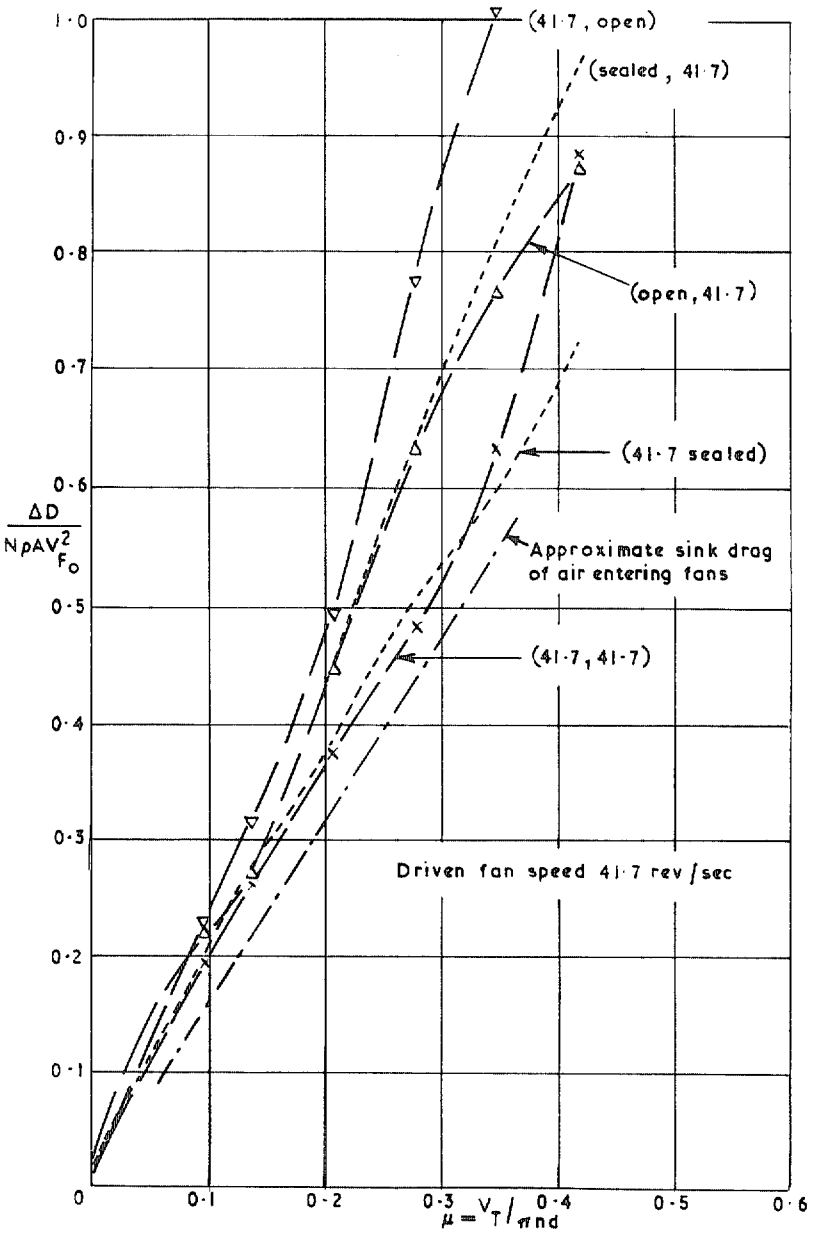

FIG. 7. Variation with advance ratio of the drag increment due to the fans measured as a proportion of the corresponding momentum flux at zero forward speed.

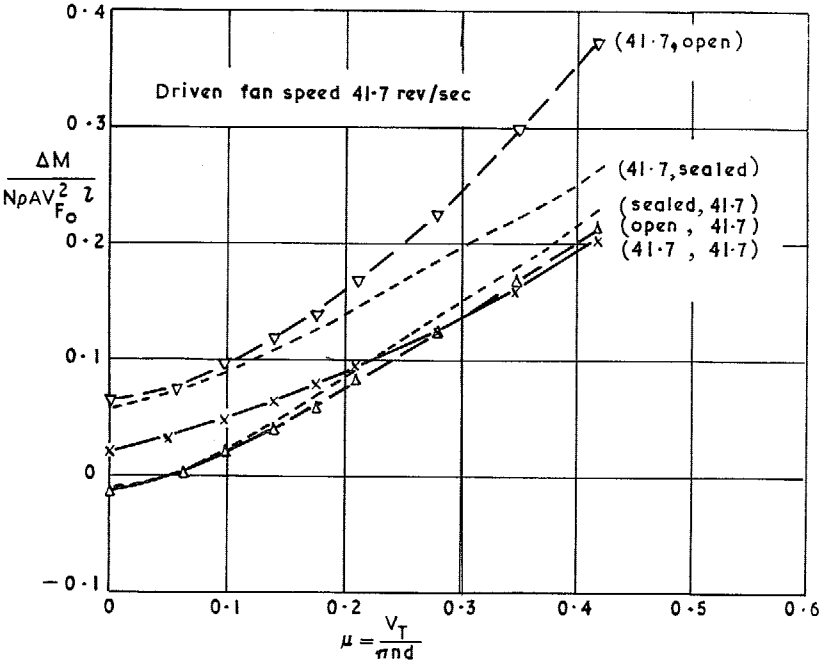

FIG. 8. Variation with advance ratio of the pitching moment increment due to the fans.

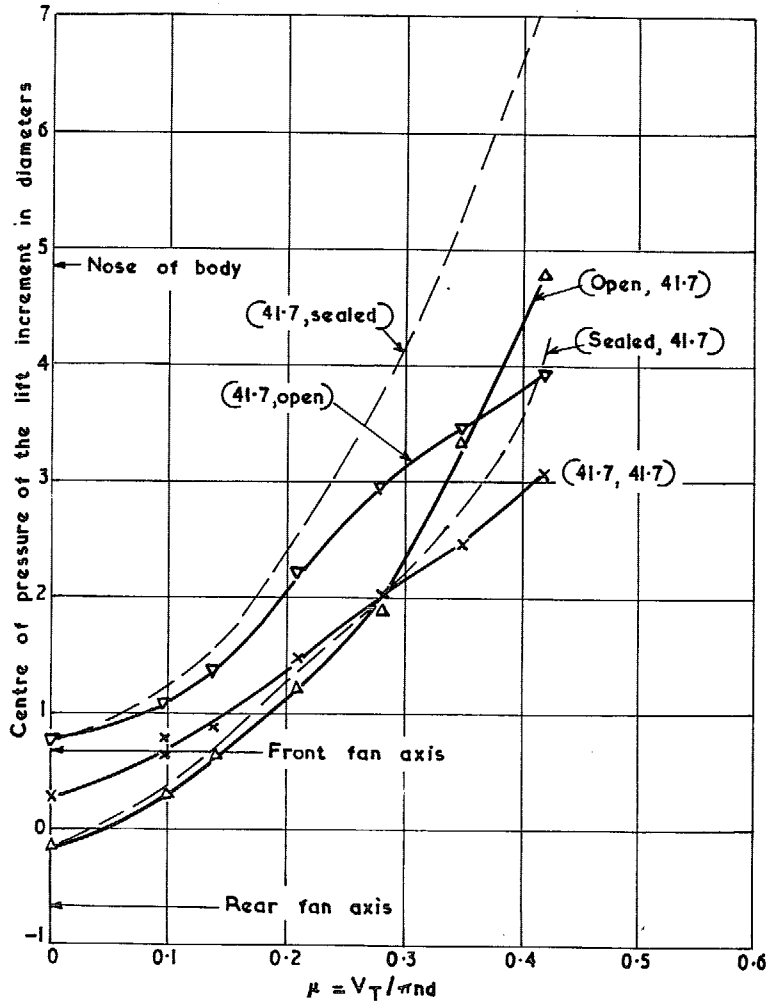

FIG. 9. Variation with advance ratio of the centre of pressure of the lift increment due to the fans, measured in fan diameters ahead of mid-fan position.

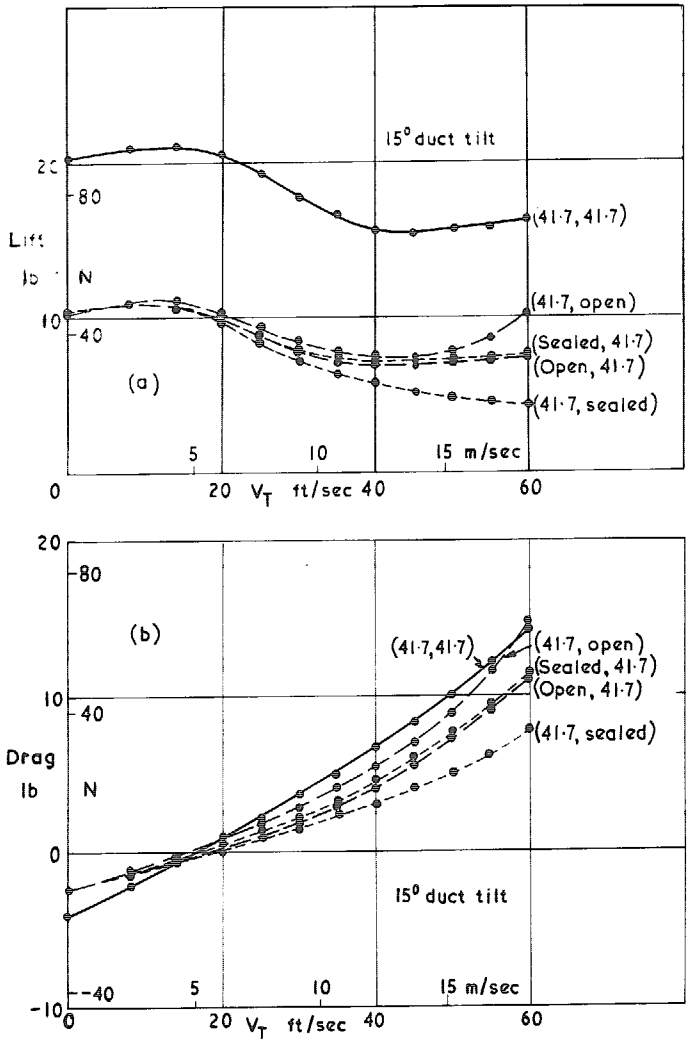

FIG. 10. Variation of (a) lift and (b) drag with forward speed for various tilted duct flow conditions. Fans either driven at 41·7 rev/sec, not driven, or duct sealed. Labels attached to curves indicate conditions at front fan and rear fan in order.

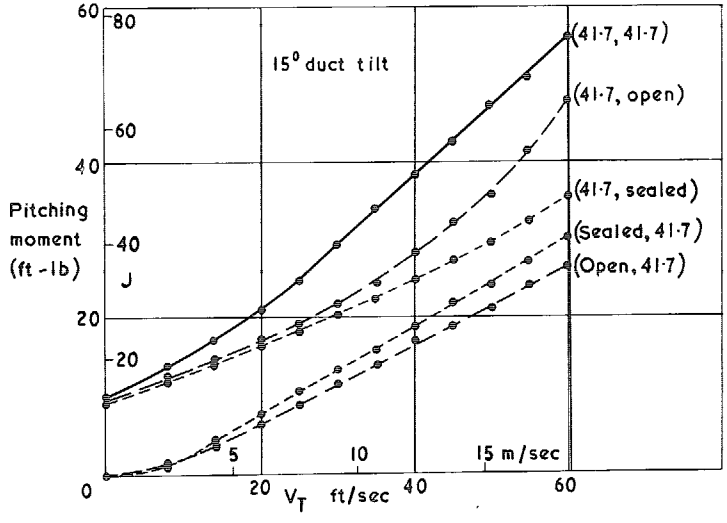

FIG. 11. Variation of pitching moment with forward speed for various tilted duct flow conditions. Fans either driven at 41·7 rev/sec, not driven, or duct sealed.

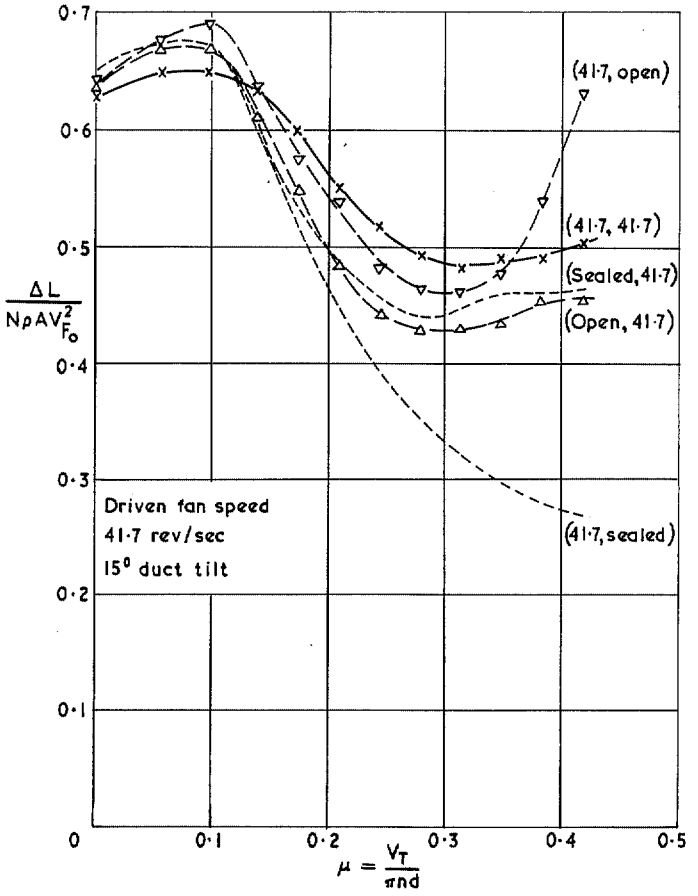

FIG. 12. Variation with advance ratio of the lift increment due to the fans, measured as a proportion of the corresponding momentum flux at zero forward speed.

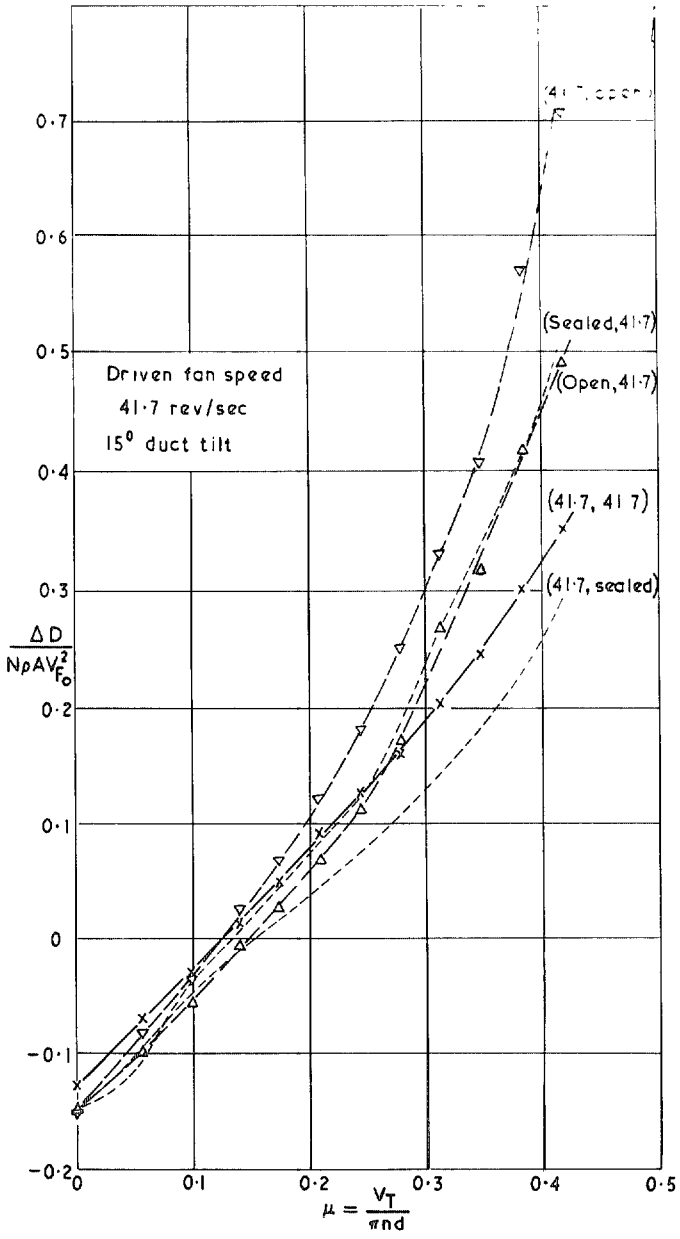

FIG. 13. Variation with advance ratio of the drag increment due to the fans measured as a proportion of the corresponding momentum flux at zero forward speed.

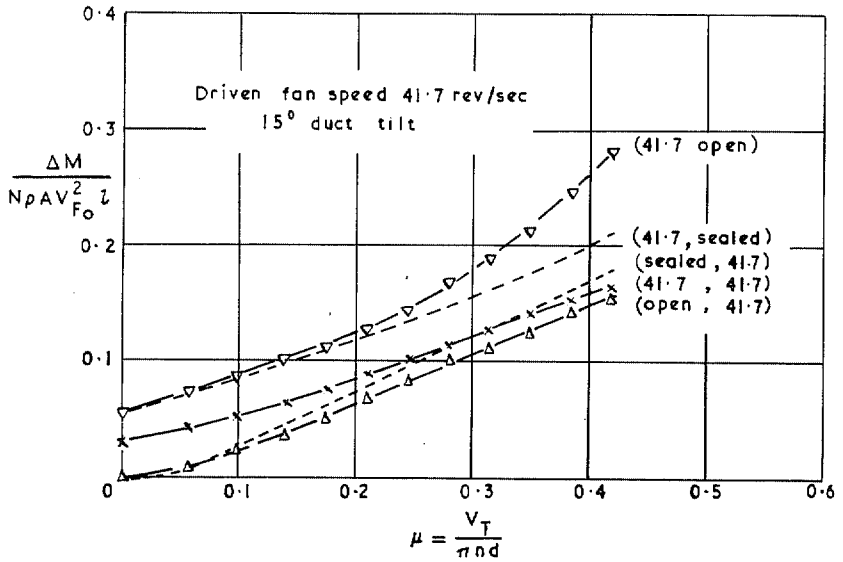

FIG. 14. Variation with advance ratio of the pitching moment increment due to the fan.

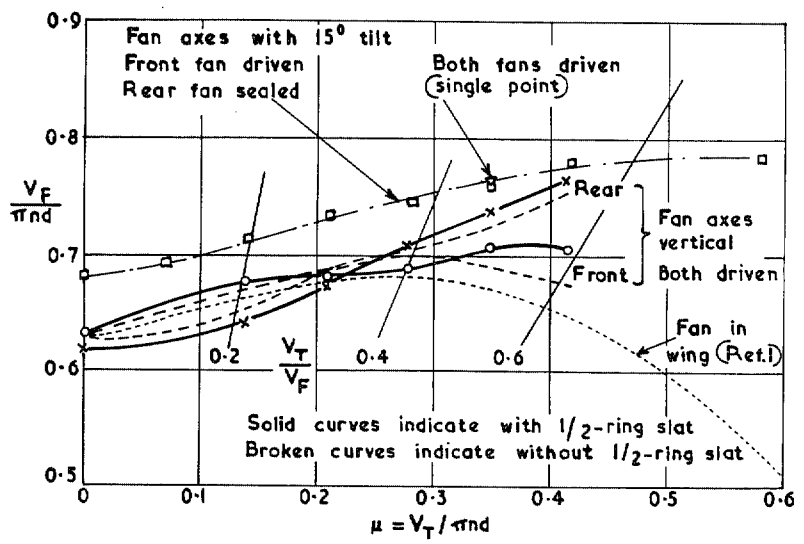

FIG. 15. Variation of fan throughput with advance ratio, for vertical and tilted fan axes.

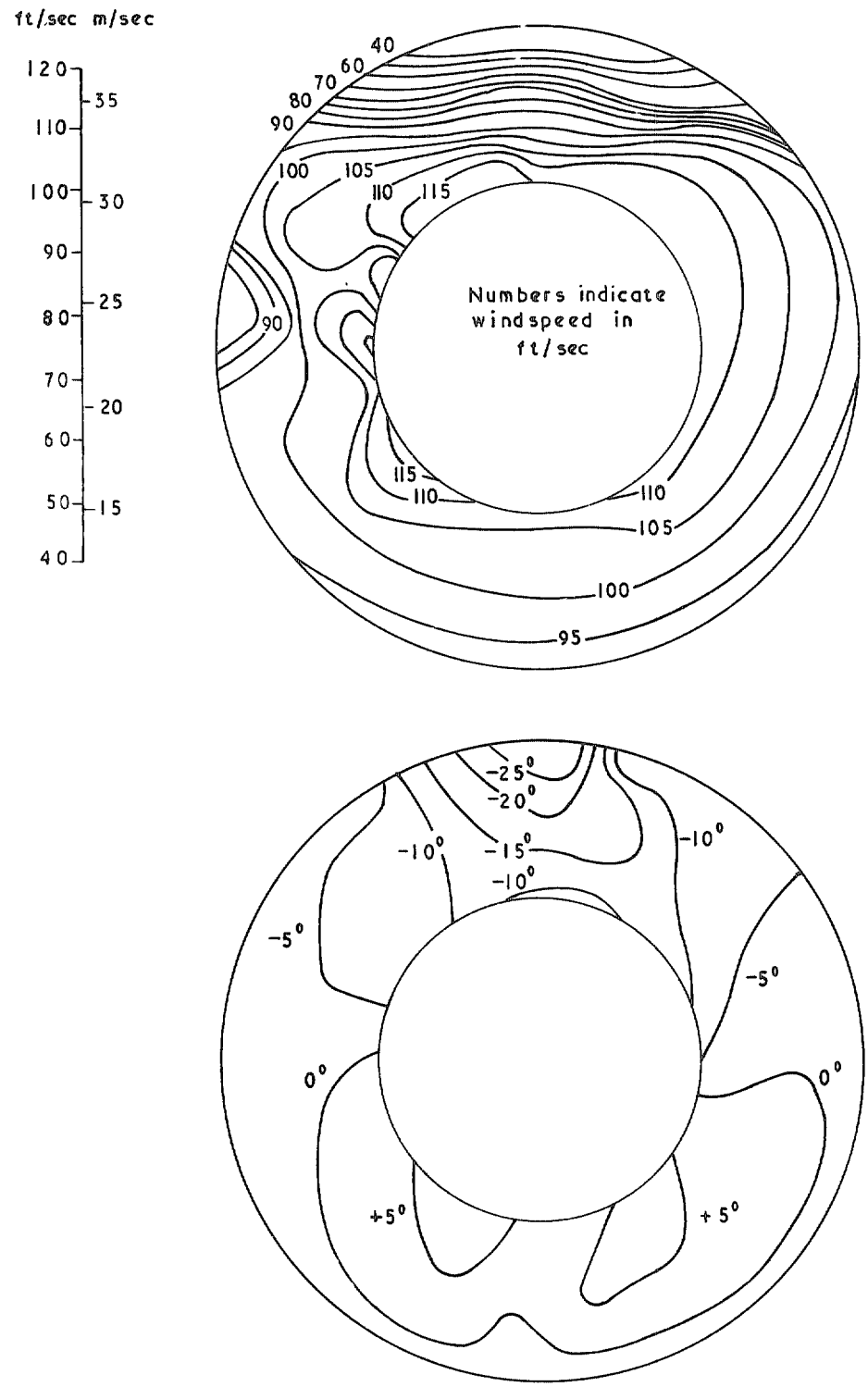

FIG. 16. Contours of equal velocity and angle of underturning for the flow into the front fan. Both fans at 41·7 rev/sec. Forward speed 50 ft/sec (15·24 m/sec). $V_T/V_F \approx 0{\cdot}48$. Traverse plane $0{\cdot}88d$ below surface.

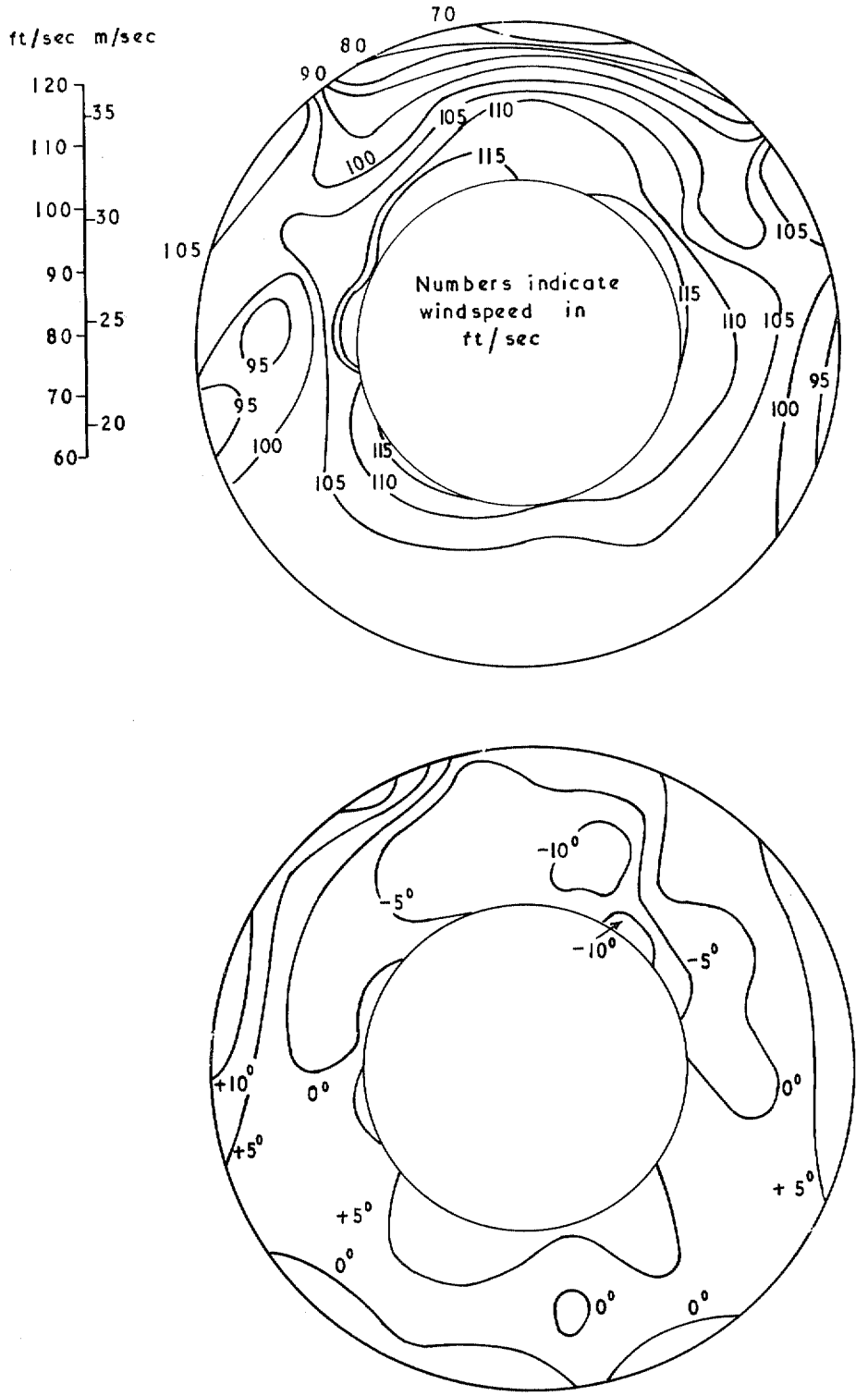

FIG. 17. Contours of equal velocity and angle of underturning for the flow into the front fan. Both fans at 41·7 rev/sec with half-ring slats fitted. Forward speed 50 ft/sec (15·24 m/sec) $V_T/V_F \approx 0{\cdot}48$. Traverse plane $0{\cdot}88d$ below surface.

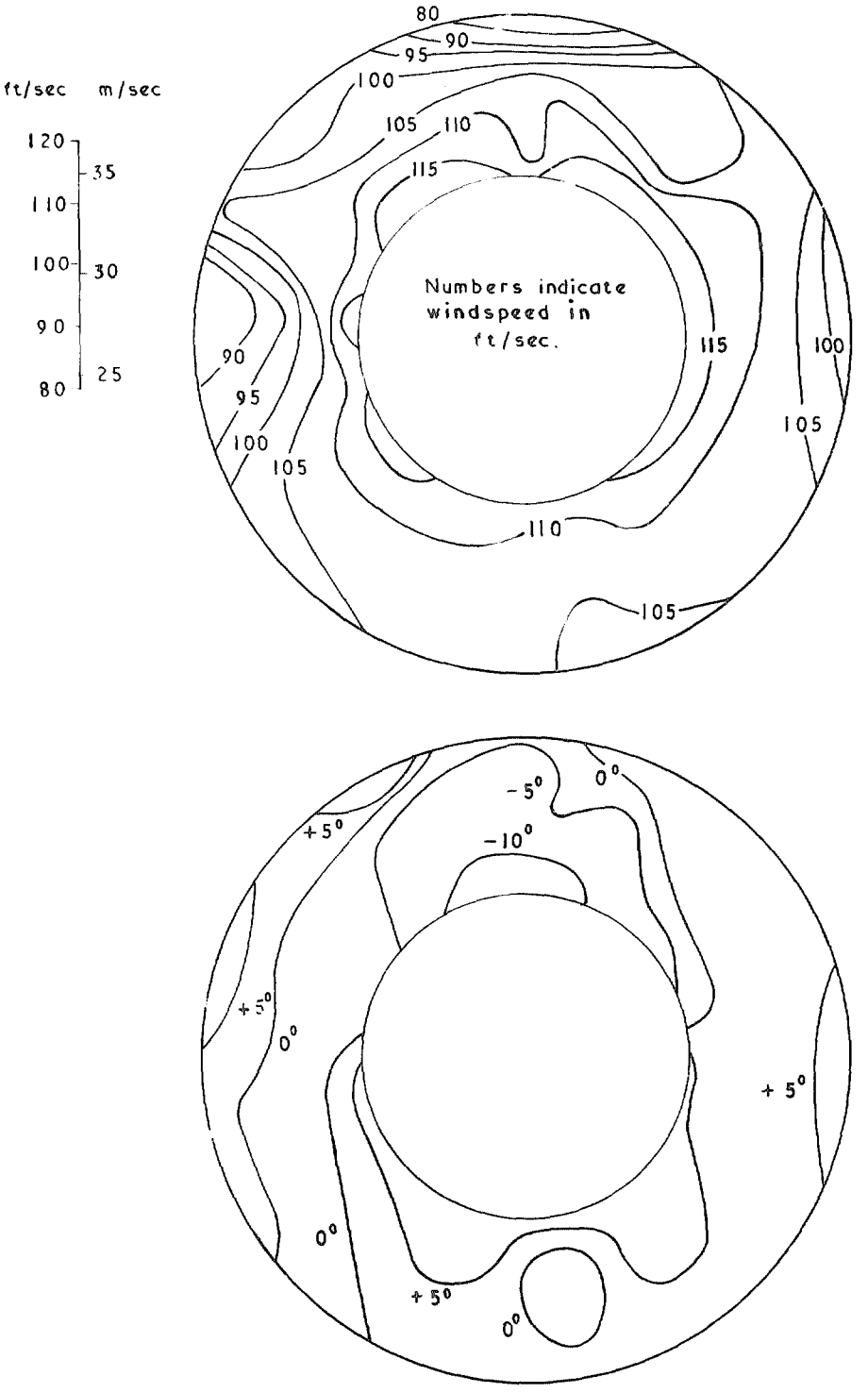

FIG. 18. Contours of equal velocity and angle of underturning for the flow into the rear fan. Both fans at 41·7 rev/sec with half-ring slats fitted. Forward speed 50 ft/sec (15·24 m/sec) $V_T/V_F \approx 0{\cdot}48$. Traverse plane $0{\cdot}88d$ below surface.

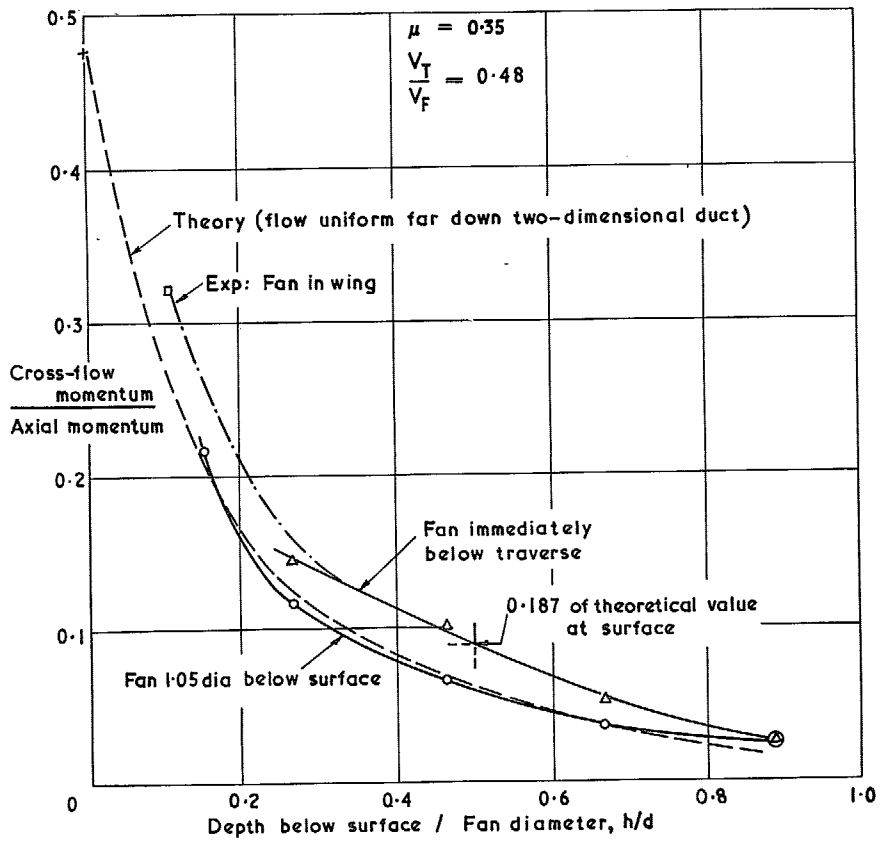

FIG. 19. Decay of cross-flow in duct perpendicular to mainflow.

Flush entry. Inlet radii: upstream, 0·23 × fan diameter
downstream, 0·115 × fan diameter.

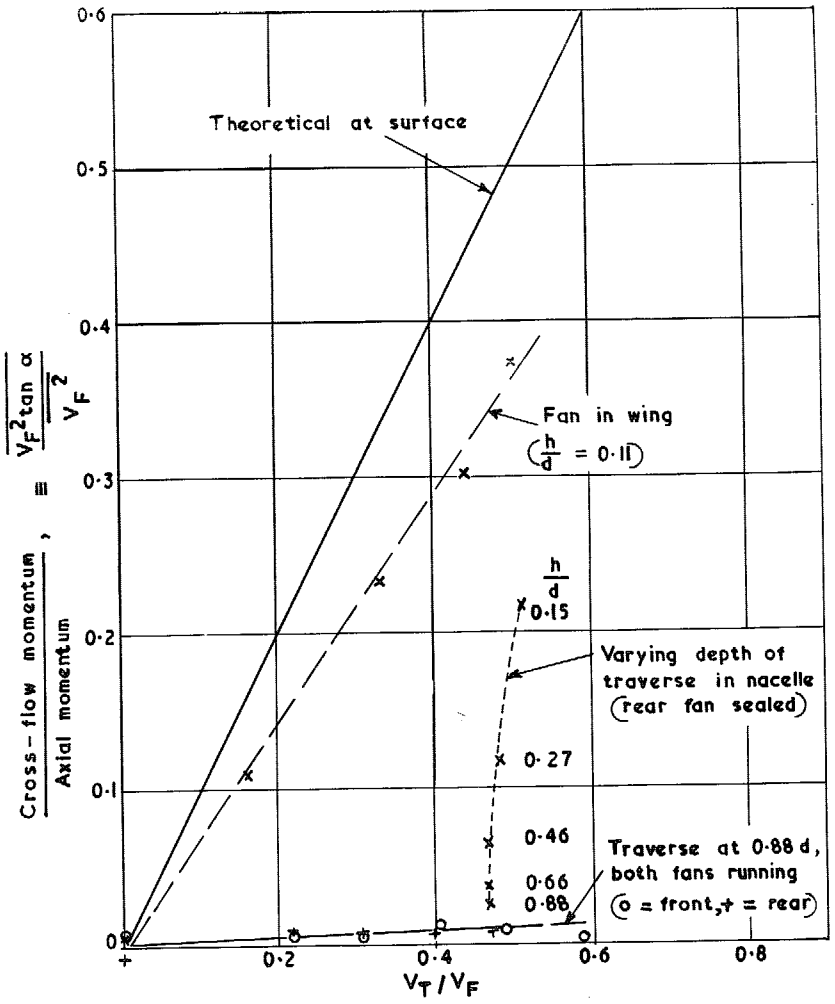

FIG. 20. Variation of cross-flow momentum with forward speed ratio and depth of traverse for fan with vertical axis in wing and nacelle.

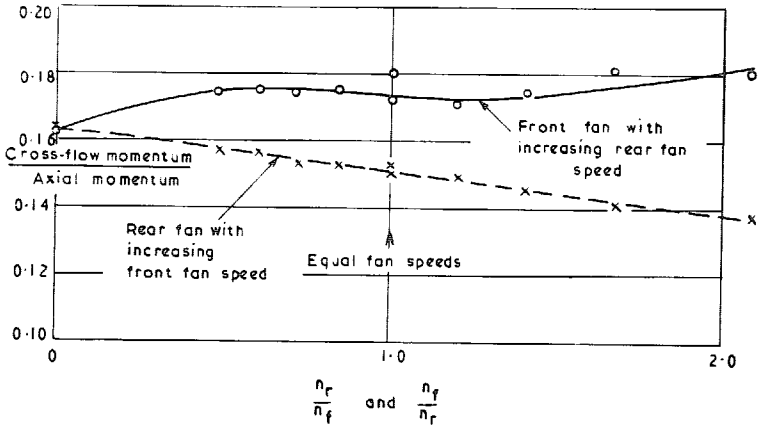

FIG. 21. Effect of variation of one fan speed on cross-flow momentum flux through other at constant rotational speed and forward velocity, $\mu = 0{\cdot}35$, $V_T/V_F = 0{\cdot}48$ approx.

Traverse at $\frac{h}{d} = 0{\cdot}27$ below surface.

Fans immediately below traverse $\left(\frac{h}{d} = 0{\cdot}43\right)$.

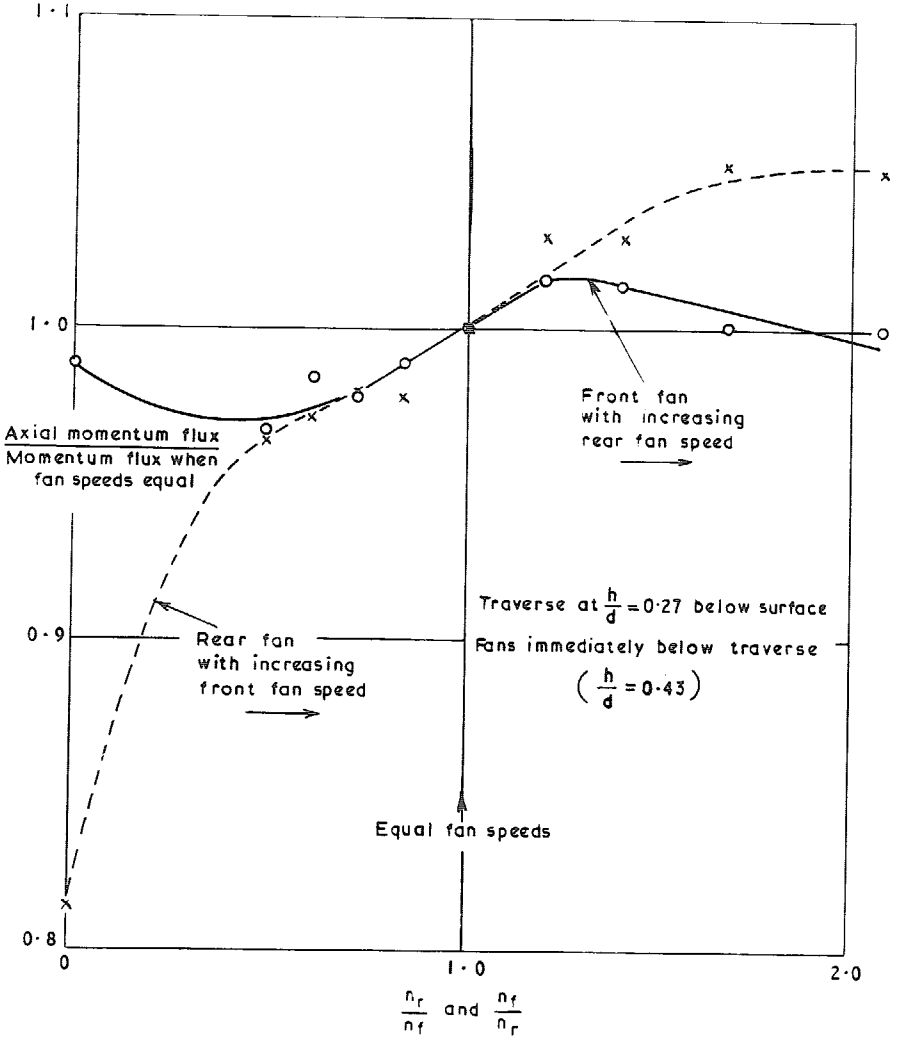

FIG. 22. Effect of variation of one fan speed on axial momentum flux through other at constant rotational speed and forward velocity, $\mu = 0{\cdot}35$, $V_T/V_F = 0{\cdot}48$ approx.

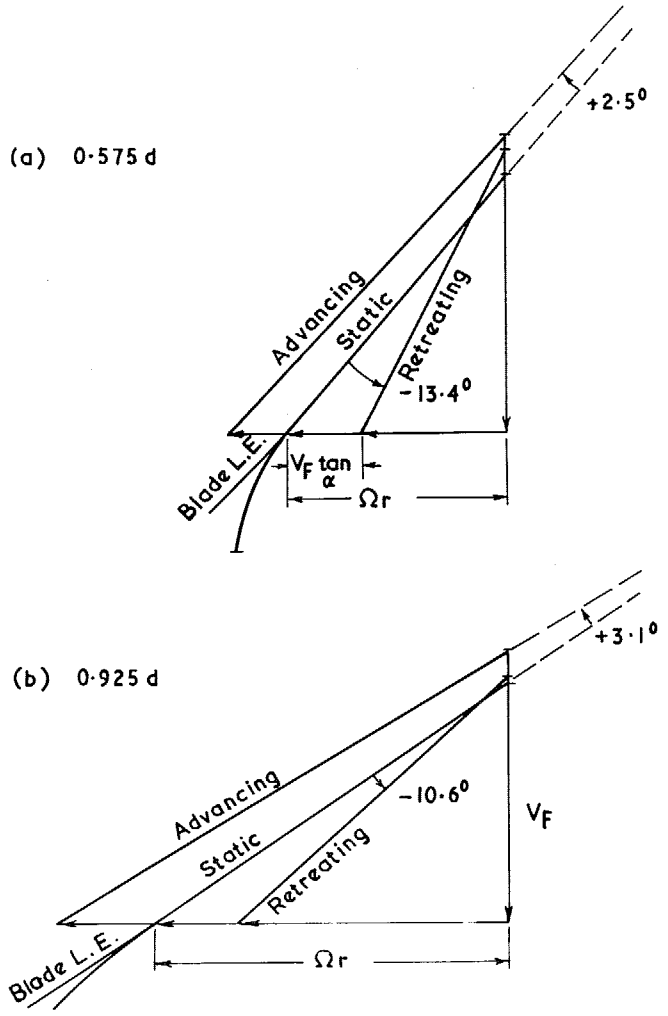

FIG. 23. Fan blade velocity triangles, (a) near root (b) near tip, for static conditions and at $V_T/V_F = 0{\cdot}48$ for fan near surface ($h/d = 0{\cdot}30$) and no inlet cascades. Triangles based on traverse at $h/d = 0{\cdot}27$ and neglecting effect of fan inlet guide vanes.

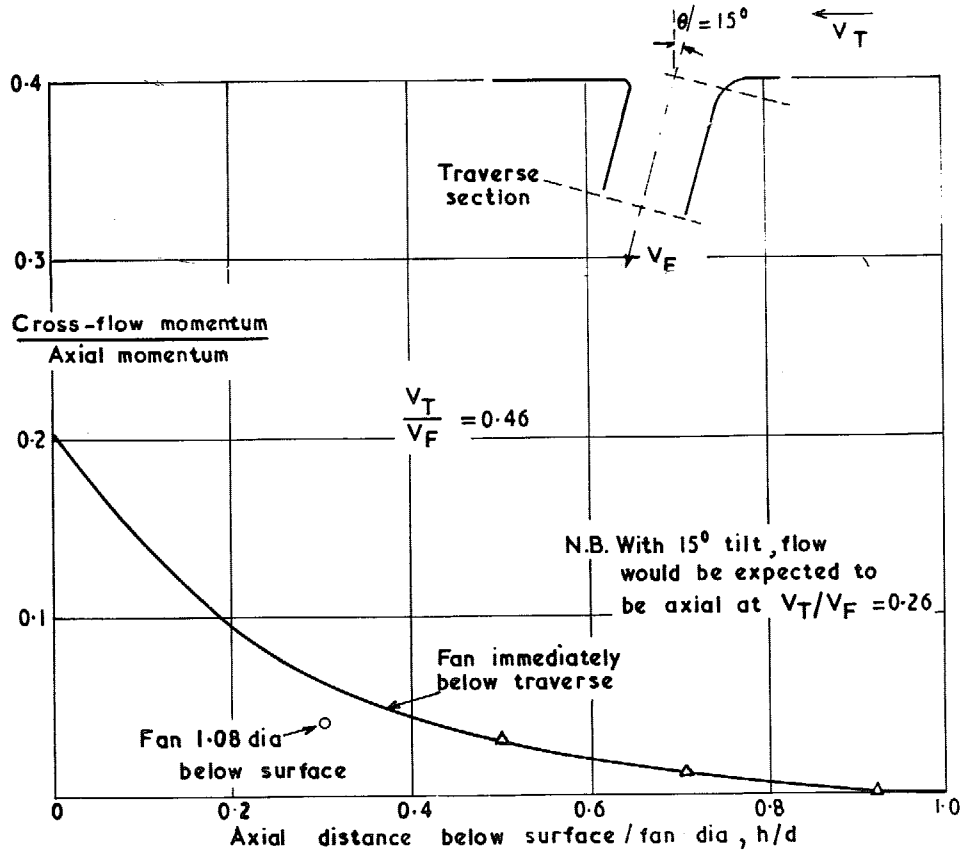

FIG. 24. Decay of cross-flow in duct tilted 15 deg to the rear at $\frac{V_T}{V_F} = 0{\cdot}46$

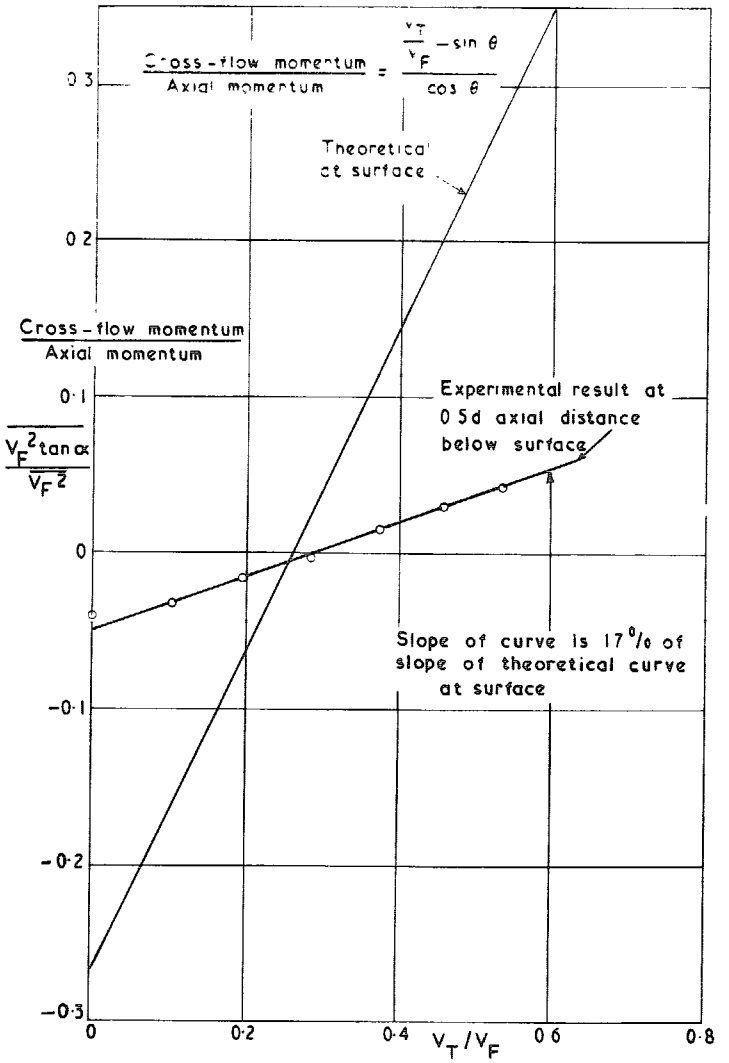

FIG. 25. Variation of cross-flow at 0·5 duct diameter below surface with forward speed for 15 deg tilted fan immediately below traverse.

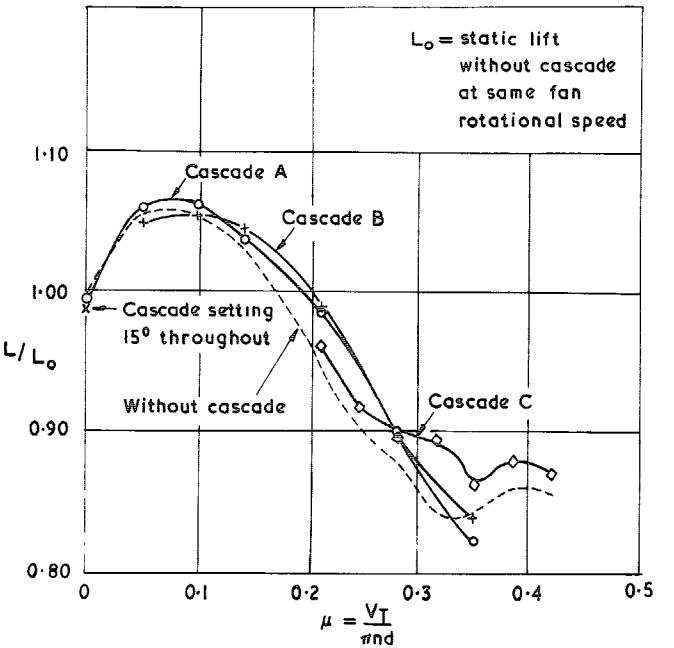

FIG. 26. Variation of lift ratio with advance ratio for various entry cascade arrangements in 15 deg tilted duct with square entry and modified square exit. Both fans driven at 41·7 rev/sec.

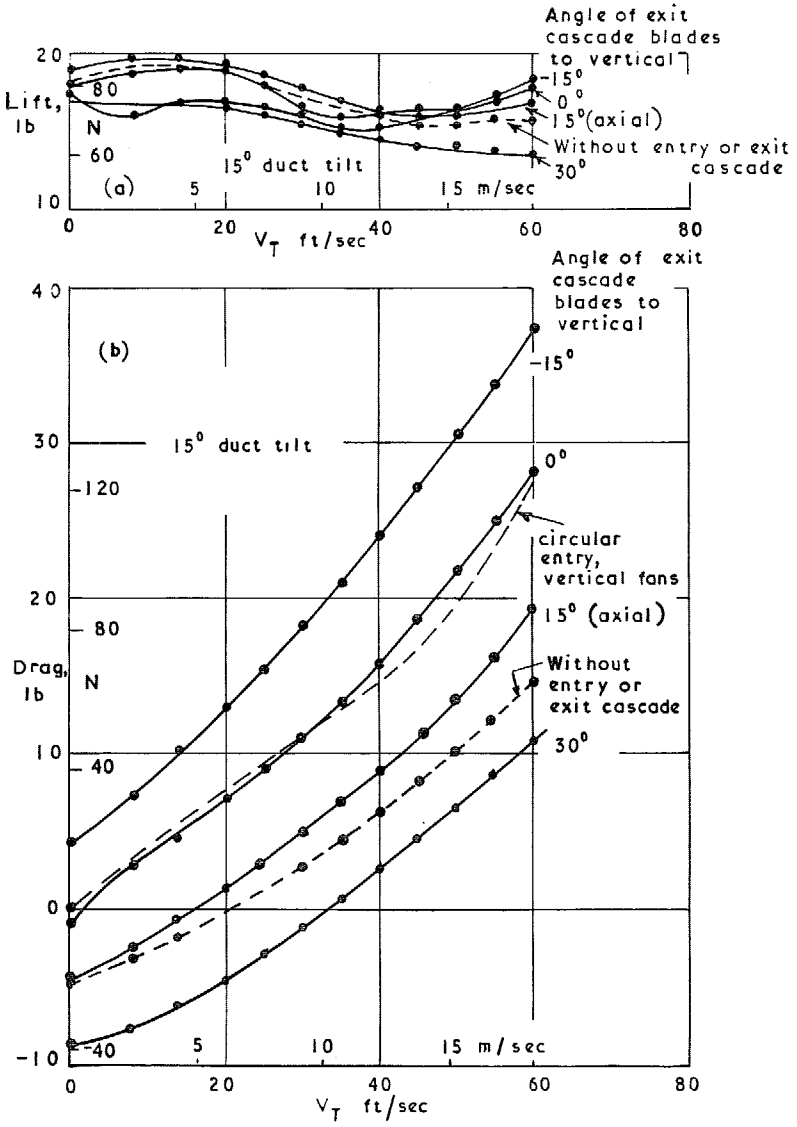

FIG. 27. Variation of (a) lift and (b) drag with forward speed for tilted ducts with optimum inlet cascade and various exit cascade deflections. Fans driven at 41·7 rev/sec.

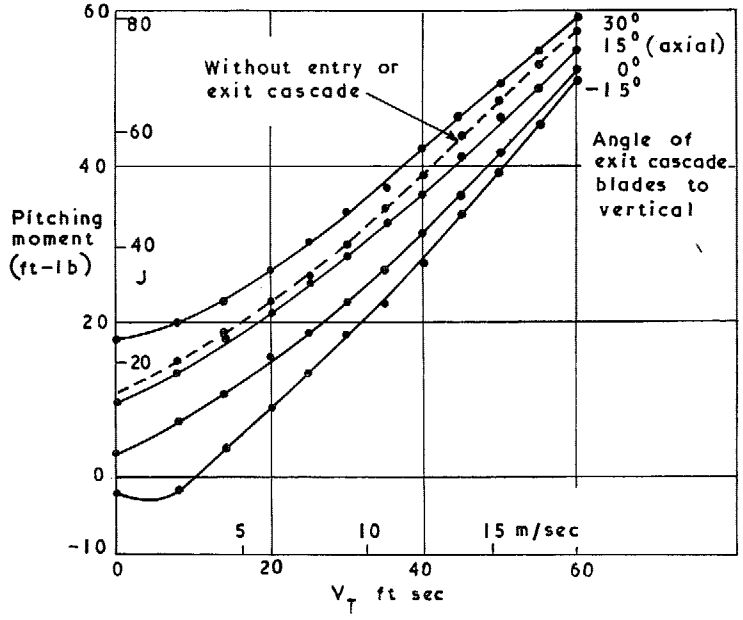

FIG. 28. Variation of pitching moment with forward speed for tilted ducts with optimum inlet cascade and various exit cascade deflections. Fans driven at 41·7 rev/sec.

Printed in Wales for Her Majesty's Stationery Office by Allens Printers (Wales) Limited.
Dd. 129527 K5.

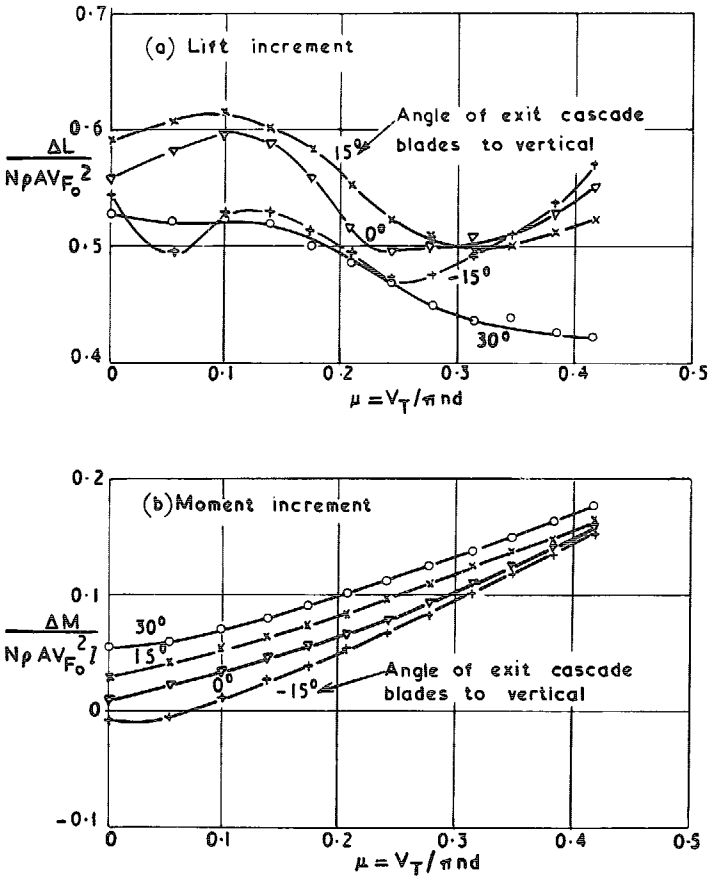

FIG. 29. Variation with advance ratio of (a) lift increment and (*b*) pitching moment increment due to the fan for filted ducts with optimum inlet cascade and various exit cascade deflections.

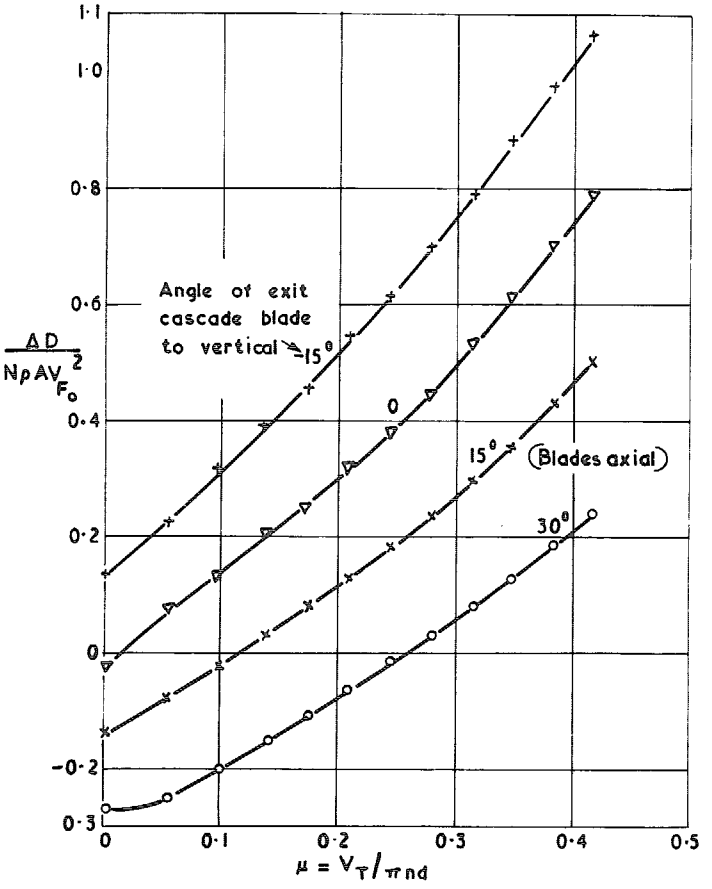

FIG. 30. Variation with advance ratio of drag increment due to the fan for tilted ducts with optimum inlet cascade and various exit cascade deflections.

Published by
HER MAJESTY'S STATIONERY OFFICE

To be purchased from
49 High Holborn, London W.C.1
423 Oxford Street, London W.1
13A Castle Street, Edinburgh 2
109 St. Mary Street, Cardiff CF1 1JW
Brazennose Street, Manchester 2
50 Fairfax Street, Bristol 1
258/259 Broad Street, Birmingham 1
7-11 Linenhall Street, Belfast BT2 8AY
or through any bookseller

S.O. Code No. 23-3494